FFI RAPPORT

Oxidation and carburisation of steel in gun barrels

FRØYLAND ØYVIND, MOXNES JOHN F.

FFI/RAPPORT-2006/03845

Oxidation and carburisation of steel in gun barrels

FRØYLAND ØYVIND, MOXNES JOHN F.

FFI/RAPPORT-2006/03845

FORSVARETS FORSKNINGSINSTITUTT
Norwegian Defence Research Establishment
P O Box 25, NO-2027 Kjeller, Norway

FORSVARETS FORSKNINGSINSTITUTT (FFI)
Norwegian Defence Research Establishment

P O BOX 25
N0-2027 KJELLER, NORWAY

UNCLASSIFIED

SECURITY CLASSIFICATION OF THIS PAGE
(when data entered)

REPORT DOCUMENTATION PAGE

1) PUBL/REPORT NUMBER	2) SECURITY CLASSIFICATION	3) NUMBER OF PAGES
FFI/RAPPORT-2006/03845	UNCLASSIFIED	51
1a) PROJECT REFERENCE	**2a) DECLASSIFICATION/DOWNGRADING SCHEDULE**	
FFI-V/860/01	-	

4) TITLE

OXIDATION AND CARBURISATION OF STEEL IN GUN BARRELS

5) NAMES OF AUTHOR(S) IN FULL (surname first)

Frøyland Øyvind, Moxnes John F.

6) DISTRIBUTION STATEMENT

Approved for public release. Distribution unlimited. (Offentlig tilgjengelig)

7) INDEXING TERMS

IN ENGLISH:	IN NORWEGIAN:
a) Oxidation	a) Oksidering
b) Carburisation	b) Karbonisering
c) Hardness	c) Hardhet
d) Carbon dioxide	d) Karbondioksid
e) Thermogravimetric analysis	e) Termogravimetrisk analyse

THESAURUS REFERENCE:

8) ABSTRACT

In this report a theoretical and experimental study of some basic gun barrel erosion mechanisms have been carried out. The theoretical analysis of the reaction mechanisms leading to erosion is based on the minimalization of Gibbs free energy. Oxygen, carbon dioxide, carbon monoxide and argon are used in a thermo gravimetric (TGA) experimental study. Based on the TGA experiments and on hardness measurements of the heat affected specimens, we suggest an explanation for the heat affected zone for the lands in a gun barrel.

In general we find that the erosion mechanisms are quite complex, but we believe that some basic insight into the more general problem of gun barrel erosion has been achieved through the theoretical and experimental study in this report.

9) DATE	AUTHORIZED BY	POSITION
	This page only	
14 December 2006	Bjarne Haugstad	Director of Research

ISBN 978-82-464-1101-9

UNCLASSIFIED

SECURITY CLASSIFICATION OF THIS PAGE
(when data entered)

CONTENTS

OXIDATION AND CARBURISATION OF STEEL IN GUN BARRELS

1 INTRODUCTION

Gun erosion has been known as an inevitable problem in use of current gun system, although extensive efforts have been paid to minimize it in the world. Gun erosion occurs as an increase in the bore diameter, allowing gas to escape past the projectile thus:

- reducing muzzle velocity
- reducing range
- reducing accuracy
- reducing penetration due to increased yaw
- increasing probability of premature during launching

In general gun barrel erosion is believed to increase the probability of premature functioning of the round both in gun barrels and outside gun barrels. A genuine understanding of the gun barrel erosion phenomenon could therefore be very profitable.

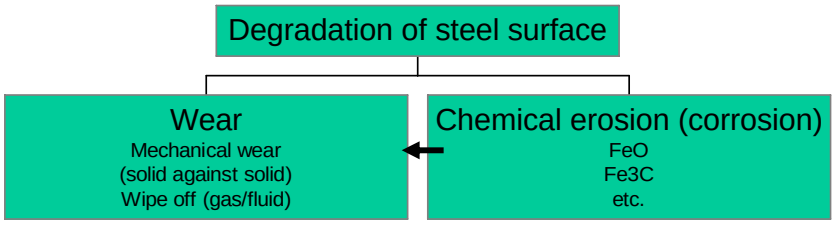

Figure 1.1: The different mechanisms

The temperature increases at the gun barrel surface is due to heat convection of the gunpowder gases, or due to mechanical friction between the projectile and the gun barrel. The two main hypotheses on the mechanisms of wear are

1. The wipe off due to heating and melting of the gun barrel surface. The heating is due to mechanical friction, inert gases or chemical reactions on the surface. The melting temperatures of the reaction products are usually lower than for steel.
2. The wipe off due to mechanical wear by high velocity gases or due to mechanical interaction. The reaction products at the surface are of a brittle nature and nearly melted. They are easily ripped off. Increased brittleness of the steel is enhancing wipe-off.

Only mechanism 2) is believed to be operative during normal situations.

The oxidation/carburisation and erosion phenomenon involves a host of different physical and chemical mechanisms and is accordingly difficult to model mathematically from first principles.

Our study starts with a short theoretical study of the composition of the gun barrel and the gunpowder gases. Having accomplished this, we perform a theoretical study on different reaction processes by using the principle of minimum Gibbs free energy. Thereafter we discuss whether a full thermodynamic equilibrium of the gunpowder gases is reached during a shot. Next we perform thermogravimetric measurements and compare with analytical theory. On doing the same for different types of gases, we identify important reaction processes. We perform hardness measurements in internal areas of the test specimen after the TGA experiment. Next, we study some different growth mechanisms of oxide layers in oxygen at 1 bar. Finally we conclude.

2 THE COMPOSITION OF THE GUN BARREL AND THE GUNPOWDER GASES

During launching different gunpowder gases interacts with the bore. Figure 2.1 shows the different mol fractions of the different gases.

Properties	Condition no. 1	6
Pressure (MPa)	53.6	431.9
Temperature (K)	2887.6	2907.6
Products	**Concentrations (mol/kg)**	
CO	18.44	18.6
H2O	9.122	9.362
H2	5.913	5.614
N2	4.569	4.543
CO2	3.923	3.711
Others	0.223	0.23
Total	42.19	42.06

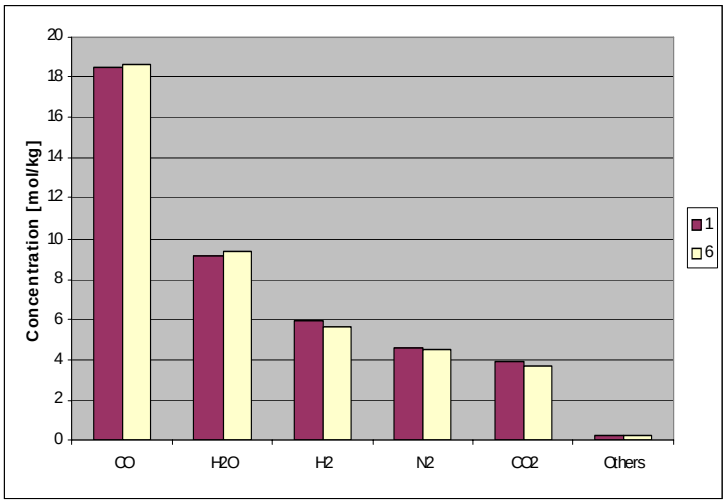

Figure 2.1: Different mol fractions of gun powder gasses from Bofors NC 1214 NEXPLO (NEXPLO). The density of the gas is 0.05 and 0.3 kg/m^3 , respectively.

During launching different gunpowder gases interact with the bore. The figures below show the different mol fractions of the reaction products calculated with the Cheetah code.

PBC 347 (lot 02SD) propellant	
Condition properties	Condition no. 6
Pressure [MPa]	430.9
Temperature [K]	2865.9
Reaction products	Concentration [mol/kg]
CO	19.49
H2O	8.74
H2	5.99
N2	4.52
CO2	3.44
Others	0.21
Total	42.38

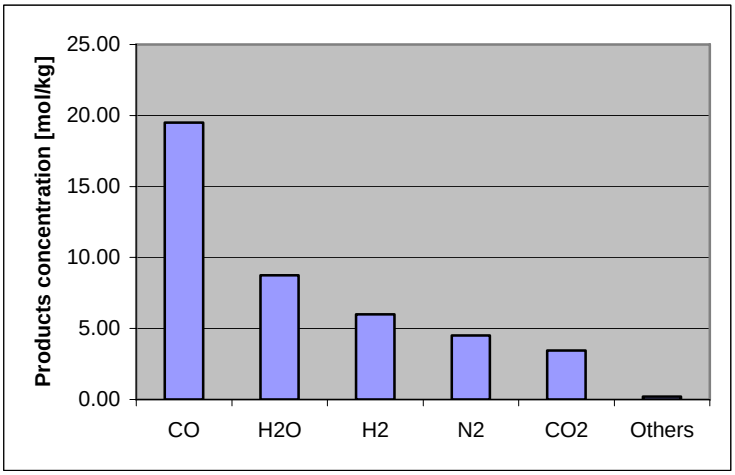

Figure 2.2: Gunpowder PBC 347 lot 02SD. The density of the gas is 0.3 kg/m^3.

PBC 347 (lot A05/00) propellant	
Condition properties	Condition no. 6
Pressure [MPa]	398.8
Temperature [K]	2479.1
Reaction products	Concentration [mol/kg]
CO	21.98
H2O	7.11
H2	8.42
N2	4.22
CO2	2.54
Others	0.33
Total	44.60

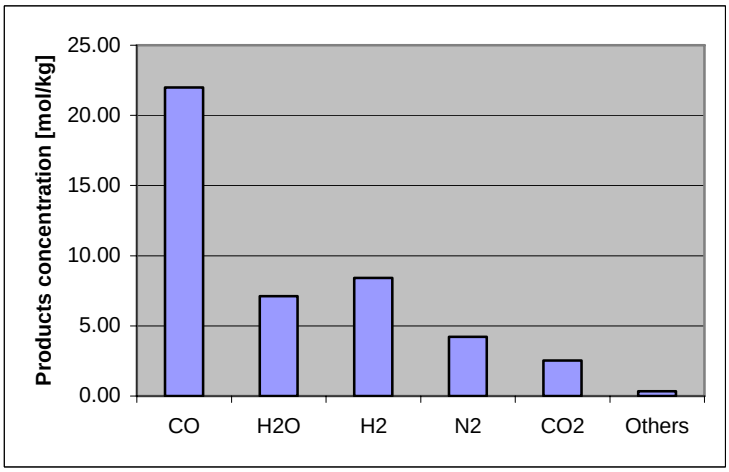

Figure 2.3: Gunpowder from PBC 347 lot A05/00. The density of the gas is 0.3 kg/m^3.

RDX/CAB propellant	
Condition properties	Condition no. 3
Pressure [MPa]	521.3
Temperature [K]	2944.9
Reaction products	Concentration [mol/kg]
CO	18.79
H2O	5.73
H2	11.33
N2	10.29
CO2	1.11
Others	0.50
Total	47.75

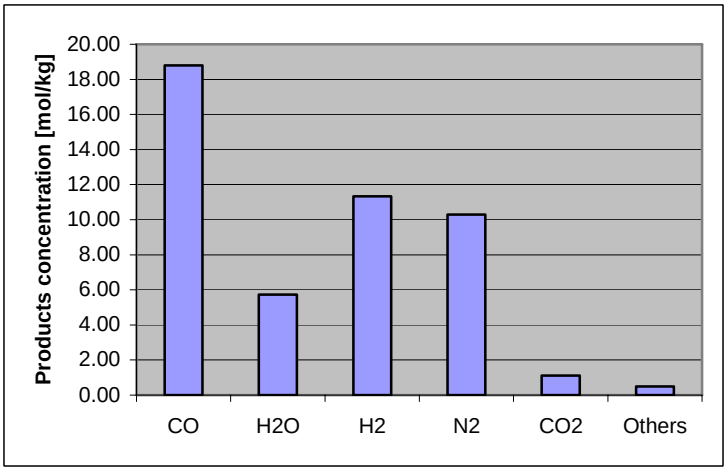

Figure 2.4: Gunpowder used for pure scientific reasons. The density of the gas is 0.3 kg/m^3.

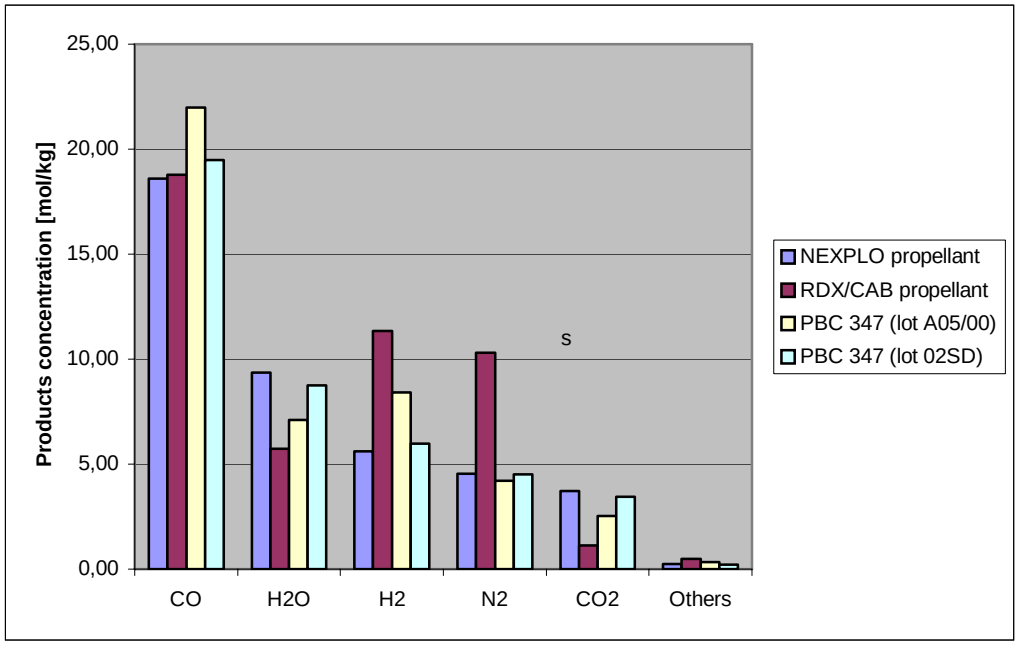

Figure 2.5: All propellants. The density of the gas is 0.3 kg/m^3.

The EDS analysis attached to the SEM instrument gives the following composition of the steel from the gun barrel. The different "alloying elements" are according to the literature too small to significantly affect the oxidation or carburisation rate of iron.

Chemical composition M2 12.7 mm gun barrel

Elements	*Atomic %*
Iron	95.97
Carbon	0.411
Chromium	1.090
Manganese	0.915
Molybdenum	0.696
Silicon	0.292
Vanadium	0.216
Nickel	0.174
Copper	0.166
Others	0.057

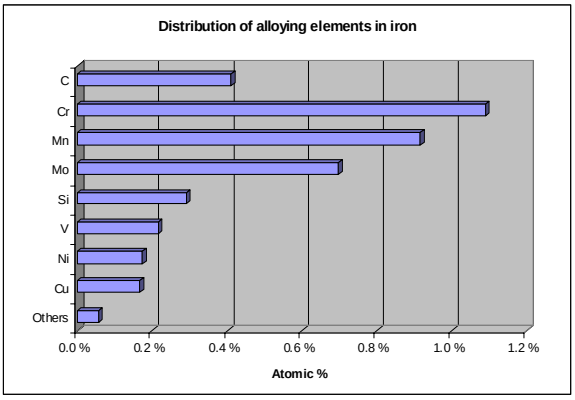

Figure 2.6: The chemical composition of the gun barrel.

The composition of the PBC 347 lot 02SD gunpowder gas was achieved by using Cheetah calculations together with the mass compositions reported from the certificate (PB Clermont in Belgium.) The composition of the PBC 347 lot A05/00 gunpowder gas was found by curve fitting the results from experimental closed bomb analyses. The composition was achieved by changing the amount of nitroglycerin and dibutylphtalate from 10.1% to 5% and 6,4% to 10% , respectively. This procedure is somewhat arbitrary.

Some more detailed physical properties of the most common reaction products in a gun barrel; wüstite (FeO) and cementite (Fe_3C), are shown in Table 2.1.

Compound	α	T_m [K]	ΔH_f [kJ/mol]	Phase transformation	ρ [kg/m3]
FeO	1.77	1630	-272	-	5700
Fe_3C	1.1	2110	25.1	-	7700
Fe	-	1810	-	$\alpha \rightarrow \gamma : 1184K$, $\gamma \rightarrow \Delta : 1665K$	7900
Melt + Fe_3C		1420			
Melt + FeO		?			

Table 2.1: Physical properties of iron and the reaction products.
α: Pilling-Bedworth ratio: the volume of the reaction products divided with the volume of the consumed metal. T_m [K]: melting temperature. ΔH_f [kJ/mol]: Heat of formation. Negative value gives exothermic reaction. ρ [kg/m3]: density.

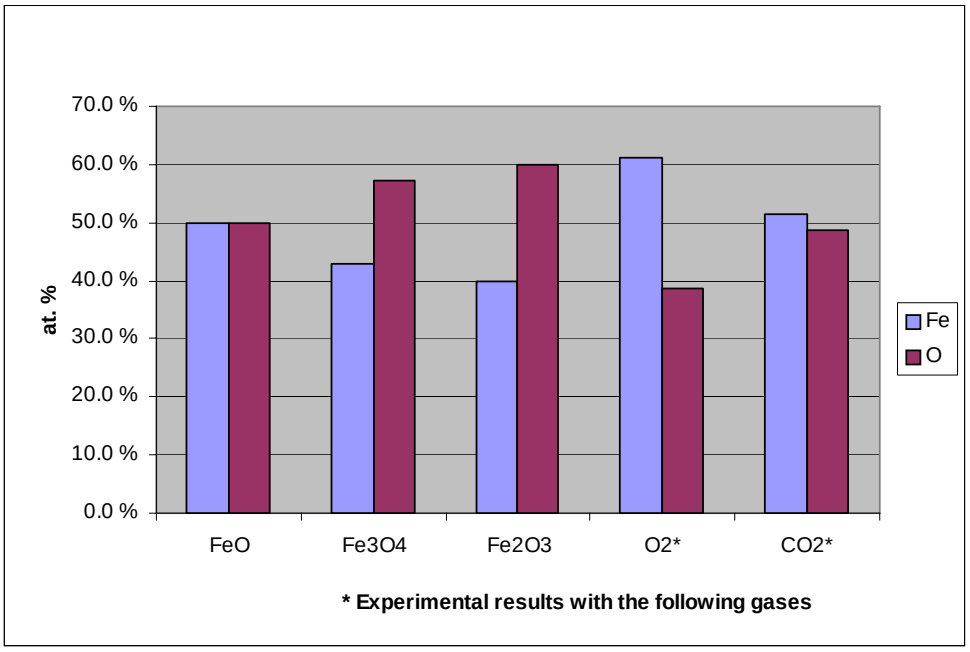

Figure 2.7: The atomic fraction of different types of oxides.

3 THERMODYNAMIC CONSIDERATIONS

A necessary condition for creating an oxide or a carbide layer is that some thermodynamic relations are fulfilled.

Consider first the fundamental reaction

$$2Fe + O_2 \underset{b}{\overset{f}{\rightleftarrows}} 2FeO \tag{3.1}$$

The reaction goes in principle forward and backward. A necessary requirement for the forward reaction is that the corresponding change in Gibbs free energy is less than zero. For isolated species we have

$$G_{O_2}(P,T,n_{O_2}) \overset{mod}{=} n_{O_2}\mu_{O_2}(P,T), \mu_{O_2} \overset{mod}{=} \mu_{O_2}{}^0(T) + RTLog\left(f\right),$$
$$f(P,T) \overset{def}{=} Exp\left(\int_{P_{ref}}^{P} \frac{V(p',T)}{n_{O_2}RT}dp'\right) \approx P/P_{ref}, P_{ref} = 1bar, \quad (3.2)$$
$$G_{Fe}(P,T,n_{Fe}) = \mu_{Fe}(T)n_{Fe}, G_{FeO}(P,T,n_{FeO}) = \mu_{FeO}(T)n_{FeO}$$

where μ refers to the chemical potential of the species, "mod" mean model assumption and "def" means definition. Observe that we have used the quite common assumption that the chemical potential of solids are independent of the pressure, and that the gas follows the ideal gas law.

The Gibbs free energy and the change in Gibbs free energy of many species systems are according to the theory of thermodynamics given as

$$G(P_{O_2},T) = \mu_{Fe}(T)n_{Fe} + \mu_{O_2}(P_{O_2},T)n_{O_2} + \mu_{FeO}(T)n_{FeO}$$
$$\Delta G = \mu_{Fe}(T)\Delta n_{Fe} + \mu_{O_2}(P_{O_2},T)\Delta n_{O_2} + \mu_{FeO}(T)\Delta n_{FeO} = \left(2\mu_{FeO}(T) - 2\mu_{Fe}(T) - \mu_{O_2}(P_{O_2},T)\right)\Delta n$$
$$= \left(\Delta G_0(T) - RTLog\left(\frac{P_{O_2}}{P_{ref}}\right)\right)\Delta n \le 0, \Delta n \ge 0, 2\mu_{FeO}(T) - 2\mu_{Fe}(T) - \mu_{O_2}{}^0(T) \overset{def}{=} \Delta G_0(T),$$
$$\Delta n \overset{def}{=} (1/2)\Delta n_{FeO}, P_{ref} = 10^5 Pa, R = 8.314 J/(kgK) \quad (3.3)$$

The reaction in equation (3.1) advance forward only if the change in Gibbs free energy is less or equal to zero, i.e. from (3.3) it follows that for the forward reaction

$$\frac{P_{O_2}}{P_{ref}} \ge Exp\left(\Delta G_0(T)/(RT)\right) = Exp\left((2\mu_{FeO}(T) - 2\mu_{Fe}(T) - \mu_{O_2}{}^0(T))/(RT)\right) \overset{def}{=} P_{O_2}^c / P_{ref} \quad (3.4)$$

Thus the pressure of oxygen must be above a certain limit, the critical pressure $P_{O_2}^c$, to advance the forward reaction. The literature gives the following equation

$$\Delta G_0(T) = \text{-528649+130.79T}, \quad 2Fe + O_2 \underset{b}{\overset{f}{\rightleftarrows}} 2FeO \quad (3.5)$$

Now we can plot the critical oxygen pressure as a function of the temperature and compare with the maximum oxygen pressure P_{O_2} during a shot. See Figure (3.1).

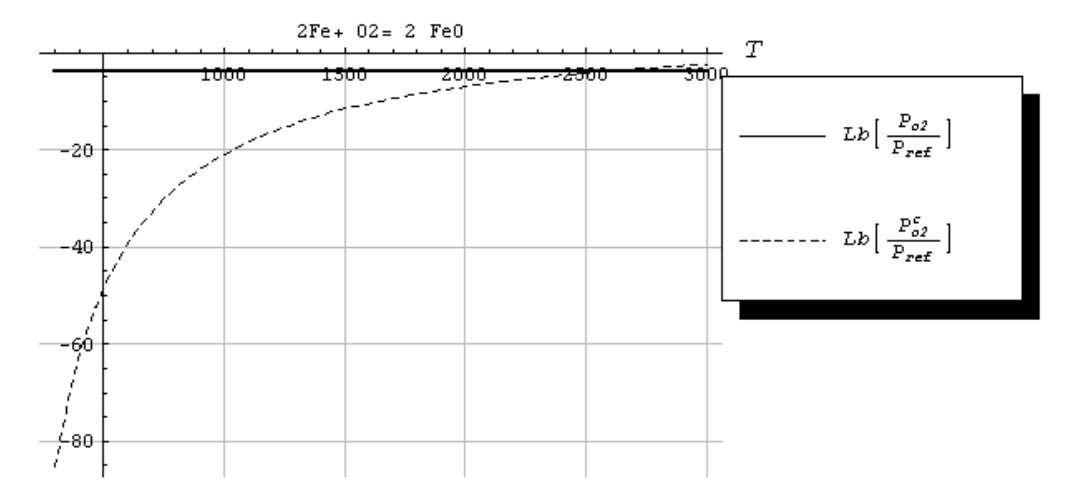

Figure 3.1: The Briggs logarithm of the relative pressure as a function of temperature T in Kelvin. P_{O_2} =14Pa. P_{ref} =1 bar. $\Delta G_0(T) = -528649+130.79T$, $2Fe + O_2 \underset{b}{\overset{f}{\rightleftarrows}} 2FeO$.

The maximum oxygen pressure P_{O_2} in the gun during firing is higher than the critical pressure for temperatures below 2500 K. Thus any wüstite layer can be formed for temperatures below 2500 K. The conclusion is not straight forward since the average temperature of the gunpowder gas is around 2900 K while the temperature of the gun barrel steel is around 1200 K as a maximum. The temperature difference tends to shift the reaction in the forward direction. More importantly, close to the steel surface the temperature of the gun barrel steel and the gunpowder gas are the same. Thus the reasonable assumption is that the temperature of the gun barrel steel surface represents the temperature of the chemical reaction.

Further, consider the following reaction

$$3Fe + C \underset{b}{\overset{f}{\rightleftarrows}} Fe_3C \tag{3.6}$$

This reaction can advance forward or backward depending on the carbon activity. We have that

$$\begin{aligned} &G(P,T) = \mu_{Fe}(T)n_{Fe} + \mu_C(a_C(P),T)n_C + \mu_{Fe_3C}(P,T)n_{Fe_3C}, \\ &\mu_C = \mu_C{}^0(T) + RTLog\left(a_C / a_{ref}\right), \\ &\Delta G(T) = \left(\mu_{Fe_3C}(T) - 3\mu_{Fe}(T) - \mu_C(a_C,T)\right)\Delta n,\ P_{ref} = 1 \text{ bar},\ a_{ref} = 1, \\ &= \left(\Delta G_0(T) - RTLog\left(\frac{a_C}{a_{ref}}\right)\right)\Delta n \le 0,\ \Delta n \ge 0,\ \mu_{Fe_3C}(T) - 3\mu_{Fe}(T) - \mu_C{}^0(T) = \Delta G_0(T), \end{aligned} \tag{3.7}$$

For the reaction to advance forward, the carbon activity must be above a critical value, to read

$$\frac{a_C^c}{a_{ref}} \ge \frac{a_C^c}{a_{ref}} = Exp\left(\Delta G_0(T)/(RT)\right) = Exp\left((\mu_{Fe_3C}(T) - 3\mu_{Fe}(T) - \mu_C{}^0(T))/(RT)\right),\ a_{ref} = 1 \tag{3.8}$$

The literature gives that

$$\Delta G_0(T) = 25873 - 22.95\,T, \quad 3Fe + C \underset{b}{\overset{f}{\rightleftarrows}} Fe_3C \tag{3.9}$$

We do not know the carbon activity during a shot, but we will now try to calculate the activity by assuming equilibrium during a shot.

Consider the two following reactions, which both give a carbon activity

$$2CO \underset{b}{\overset{f}{\rightleftarrows}} CO_2 + C, \Delta G_0(T) = -172670 + 175.94\,T, \quad (a)$$

$$CO + H_2 \underset{b}{\overset{f}{\rightleftarrows}} H_2O + C, \Delta G_0(T) = \text{Interpolation}[\{\{300,-99500\}, \quad (3.10)$$

$$\{1500,141500\},\{3000,337000\}\},\text{InterpolationOrder->1}], \quad (b)$$

Thus during equilibrium, where $\Delta G = 0$, it follows that

$$\frac{\left(a_{C1}/a_{ref}\right)\left(P_{CO_2}/P_{ref}\right)}{\left(P_{CO}/P_{ref}\right)^2} = Exp\left(-\Delta G_0(T)/(RT)\right), \Delta G_0(T) = -172670 + 175.94\,T, (a)$$

$$\frac{\left(a_{C2}/a_{ref}\right)\left(P_{H_2O}/P_{ref}\right)}{\left(P_{CO}/P_{ref}\right)\left(P_{H_2}/P_{ref}\right)} = Exp\left(-\Delta G_0(T)/(RT)\right), \Delta G_0(T) = \text{Interpolation}[\{\{300,-99500\}, \tag{3.11}$$

$$\{1500,141500\},\{3000,337000\}\},\text{InterpolationOrder->1}],(b)$$

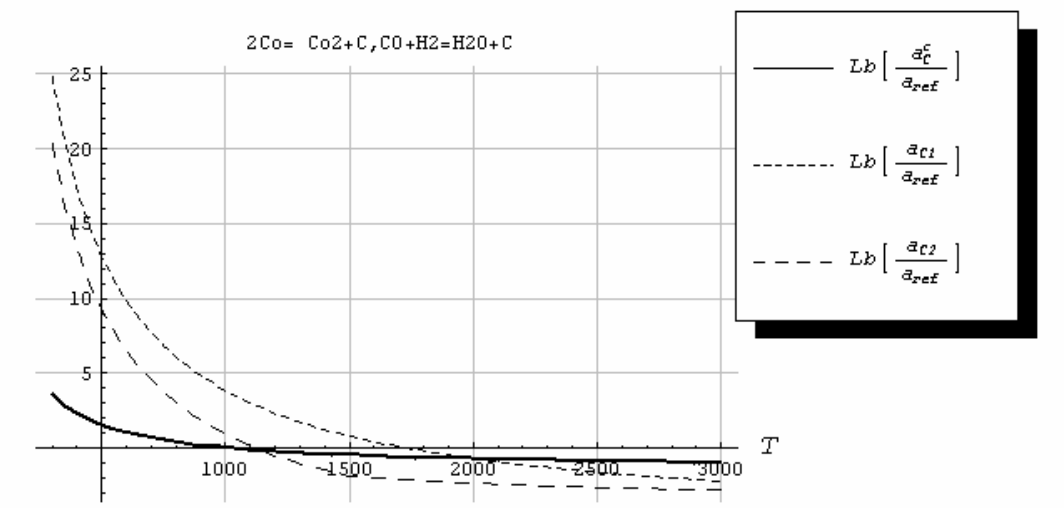

Figure 3.2: The Briggs logarithm of the activity as a function of temperature T in Kelvin. $a_{ref}=1$. a_{C1} *and* a_{C2} *are given by (3.11) ,* a_C^c *is given from equation (3.8) and (3.9).*

$P_{CO} = 1.910^8\,Pa$, $P_{CO_2} = 3.88\,10^7\,Pa$, $P_{H_2O} = 9.48\,10^7\,Pa$, $P_{H_2} = 5.6\,10^7\,Pa$.

Figure (3.2) shows the critical activity necessary to create the carbide layer and the activity according to equation (3.11). We have inserted the maximum pressures for carbon monoxide, carbon dioxide and water vapour during a shot. Thermodynamic calculations have shown that the fractions

of the different gases change insignificantly during a shot. Also the temperature is not changing very much. Thus equation (3.11) shows that the activity is almost proportional with the pressure during a shot. Reducing the pressure with a factor of ten does not change the overall conclusion in Figure 3.2, i.e., the activity during a shot is high enough to give iron carbide if the temperature is below 2000 K. In addition the activity is higher than one for temperatures below 1200 K. This suggests that even carbon deposition on the metal surface may take place.

Although the activity is high enough to create iron carbide, this does not mean that iron carbide is the thermodynamic most stable product, or more precisely the final reaction product. We may also examine the reaction

$$Fe_3C + (3/2)O_2 \underset{b}{\overset{f}{\rightleftarrows}} 3FeO + C \tag{3.12}$$

Thus if the oxygen pressure is high enough the carbide will be transformed to oxide. During equilibrium it follows readily that the critical activity is

$$\frac{a_C^{c'}}{a_{ref}} = \frac{{P_{O_2}}^{3/2}}{{P_{ref}}^{3/2}} Exp\left(\Delta G_0(T)/(RT)\right), \Delta G_0(T) = 818056 - 224.37\,T \tag{3.13}$$

Thus if the actual activity during a shot is such that $a_C \le a_C^{c'}$, the carbide will be converted to oxide in the long run. Figure (3.3) shows a plot of the situation

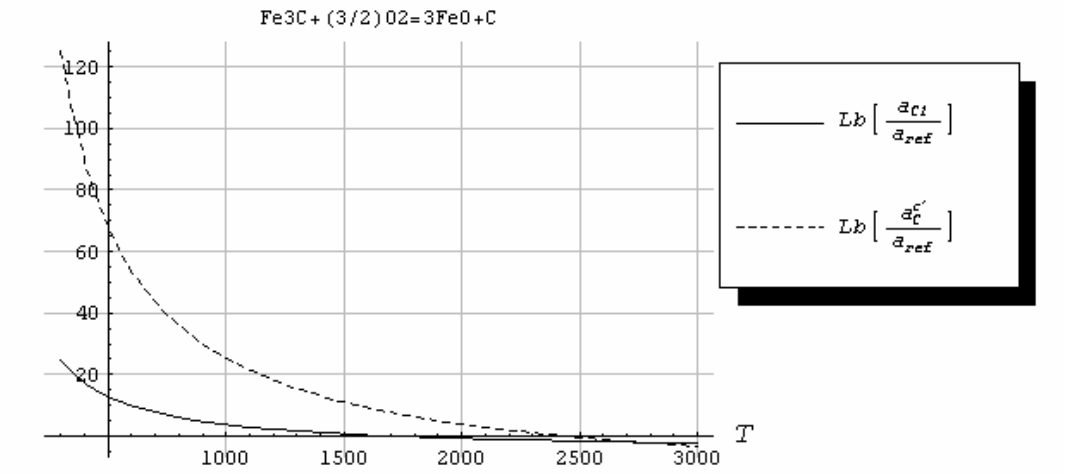

Figure 3.3: The Briggs logarithm of the relative activity as a function of temperature T in Kelvin. $P_{CO} = 1.910^8\,Pa,\ P_{CO_2} = 3.88\,10^7\,Pa,\ P_{H_2O} = 9.48\,10^7\,Pa,\ P_{H_2} = 5.6\,10^7\,Pa,\ P_{O_2} = 14$ Pa, $a_{ref} = 1,\ a_C^{c'}$ is given by equation (3.13), a_{C1} is given by equation (3.11a).

Figure 3.3 shows that the activity is lower than the critical value in (3.13). Thereby the carbide will be transformed to oxide in the long run, assuming all other conditions being constant.

We now consider the following reactions:

$$
\begin{aligned}
&Fe + CO_2 \underset{b}{\overset{f}{\rightleftarrows}} FeO + CO, (a)\\
&Fe + H_2O \underset{b}{\overset{f}{\rightleftarrows}} FeO + H_2, (b)\\
&Fe + CO \underset{b}{\overset{f}{\rightleftarrows}} FeO + C, (c)\\
&2Fe + CO_2 \underset{b}{\overset{f}{\rightleftarrows}} 2FeO + C, (d)\\
&4Fe + CO \underset{b}{\overset{f}{\rightleftarrows}} FeO + Fe_3C, (e)\\
&(5/2)Fe + CO \underset{b}{\overset{f}{\rightleftarrows}} FeO + (1/2)Fe_3C + (1/2)C, (f)\\
&5Fe + CO_2 \underset{b}{\overset{f}{\rightleftarrows}} 2FeO + Fe_3C, (g)\\
&(7/2)Fe + CO_2 \underset{b}{\overset{f}{\rightleftarrows}} 2FeO + (1/2)Fe_3C + (1/2)C, (h)
\end{aligned}
\tag{3.14}
$$

Based on thermodynamic considerations, only a, b, c and d are possible reactions.

Consider as an example the first reaction, to read

$$Fe + CO_2 \underset{b}{\overset{f}{\rightleftarrows}} FeO + CO \tag{3.15}$$

The reaction goes forward and backward. A necessary requirement for the forward reaction is that the change in Gibbs free energy is negative. Thus

$$
\begin{aligned}
&G(P,T) = \mu_{Fe}(T)n_{Fe} + \mu_{CO_2}(P_{CO_2},T)n_{CO_2} + \mu_{FeO}(T)n_{FeO} + \mu_{CO}(P_{CO},T)n_{CO}\\
&\mu_{CO_2} = {\mu_{CO_2}}^0(T) + RTLog\left(P_{CO_2}/P_{ref}\right), \mu_{CO} = {\mu_{CO}}^0(T) + RTLog\left(P_{CO}/P_{ref}\right)\\
&P_{CO_2} = Pn_{CO_2}/(n_{CO_2} + n_{CO}), P_{CO} = Pn_{CO}/(n_{CO_2} + n_{CO}), P_{ref} = 1bar
\end{aligned}
\tag{3.16}
$$

The change in Gibbs free energy is given as

$$
\begin{aligned}
&\Delta G = \mu_{Fe}(T)\Delta n_{Fe} + \mu_{CO_2}(P_{CO_2},T)\Delta n_{O_2} + \mu_{FeO}(T)\Delta n_{FeO} + \mu_{CO}(P_{CO},T)\Delta n_{CO}\\
&= \left(\mu_{FeO}(T) + \mu_{CO}(P_{CO},T) - \mu_{Fe}(T) - \mu_{CO_2}(P_{CO_2},T)\right)\Delta n\\
&= \left(\Delta G_0(T) - RTLog\left(\frac{P_{CO_2}}{P_{CO}}\right)\right)\Delta n \le 0, \Delta n \ge 0, \mu_{FeO}(T) + {\mu_{CO}}^0(T) - \mu_{Fe}(T) - {\mu_{CO_2}}^0(T) = \Delta G_0(T)
\end{aligned}
\tag{3.17}
$$

Thus the reaction advance forward only if

$$\frac{P_{CO_2}}{P_{CO}} \ge Exp\left(\Delta G_0(T)/(RT)\right) = \frac{P^c_{CO_2}}{P^c_{CO}} = Exp\left(\left(\mu_{FeO}(T) + {\mu_{CO}}^0(T) - \mu_{Fe}(T) - {\mu_{CO_2}}^0(T)\right)/(RT)\right) \tag{3.18}$$

The literature gives that

$$\Delta G_0(T) = \text{Interpolation}[\{\{100,12502\},\{200,12516\},\{300,11433\},\{400,9769\},\{500,7780\},\{600,5602\},\{700,3321\},\{800,1001\},\{900,-1300\},\{1000,-3521\},\{1100,-5599\},\{1200,-7587\},\{1300,-9514\}\},\text{InterpolationOrder->1}], \quad (3.19)$$

$$Fe + CO_2 \underset{b}{\overset{f}{\rightleftarrows}} FeO + CO$$

The critical relation can be plotted together with the relations in the gun barrel to give

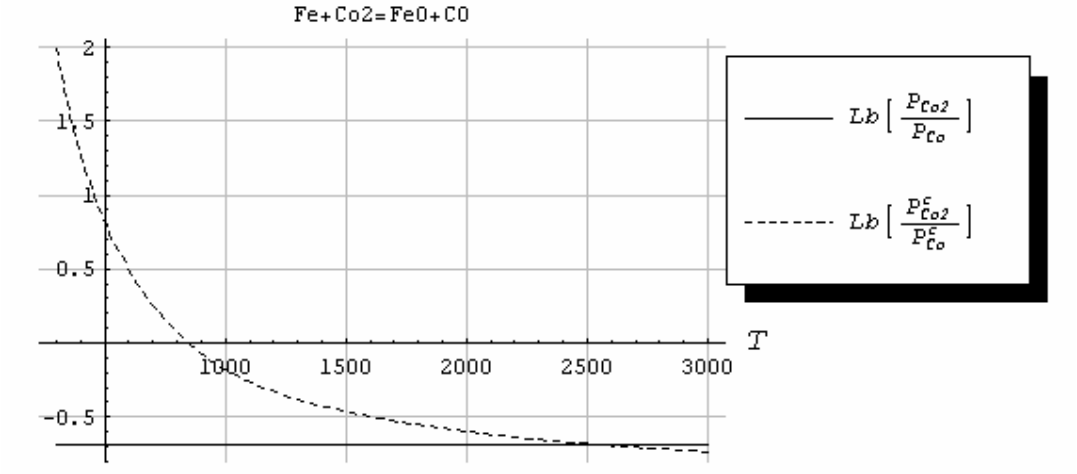

Figure 3.4: The Briggs logarithm of the relative pressure as a function of temperature T in Kelvin. $P^c_{CO_2} / P^c_{CO}$ *is given by equation (3.18),* $P_{CO} = 1.910^8\, Pa$, $P_{CO_2} = 3.88\,10^7\, Pa$.

Thus only for temperatures above 2500 K will the oxidation take place. The conclusion is that the reaction is not feasible during a shot.

Further, consider the reaction

$$Fe + H_2O \underset{b}{\overset{f}{\rightleftarrows}} FeO + H_2,$$

$$\Delta G_0(T) = \text{Interpolation}[\{\{\ 100,-24257\},\{200,-20235\},\{300,-17091\},\{400,-14622\},\{500,-12638\},\{600,-11009\},\{700,-9642\},\{800,-8458\},\{900,-7387\},\{1000,-6352\},\{1100,-5276\},\{1200,-4201\},\{1300,-3144\},\{1400,-2191\},\{1500,-1328\},\{1600,-543\},\{1700,-570\},\{1800,-1331\},\{1900,-1463\},\{2000,-1536\}\},\text{InterpolationOrder->1}] \quad (3.20)$$

The reaction advances forward only if

$$\frac{P_{H_2O}}{P_{H_2}} \geq Exp\left(\Delta G_0 /(RT)\right) = \frac{P^c_{H_2O}}{P^c_{H_2}},\ \mu_{FeO}(T) + {\mu_{H_2}}^0(T) - \mu_{Fe}(T) - {\mu_{H_2O}}^0(T) = \Delta G_0(T), \quad (3.21)$$

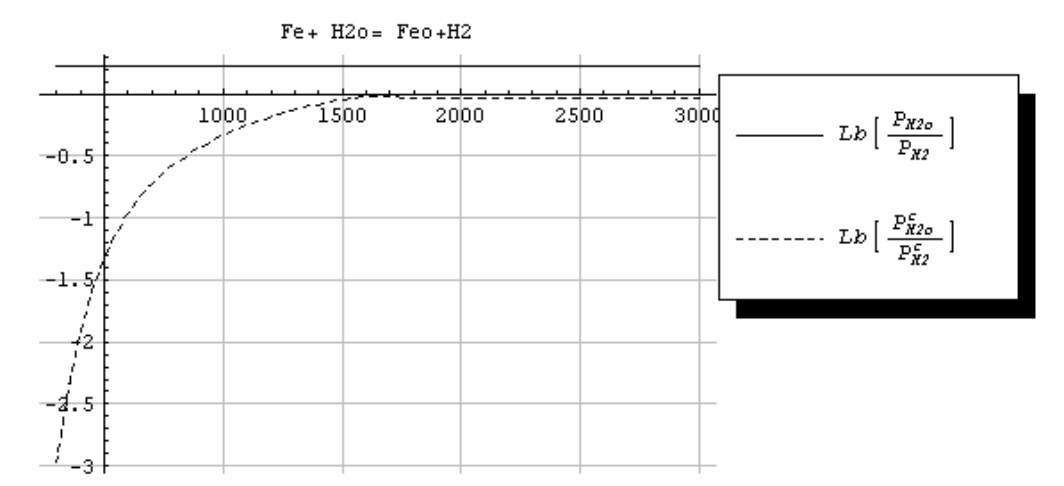

Figure 3.5: The Briggs logarithm of the relative pressure as a function of temperature T in Kelvin. $P^c_{H_2O} / P^c_{H_2}$ *is given by equation (3.21).* $P_{H_2O} = 9.48\,10^7\,Pa$, $P_{H_2} = 5.6\,10^7\,Pa$.

We observe that the reaction clearly advances forward with a quite large heat output for all temperatures. It could be beneficial to increase the hydrogen concentration in order to reverse the reaction somewhat, but this will lead to larger heat flux into the gun barrel steel due to the high conductivity of hydrogen. Thus there is a trade-off.

Moving on to the carbide formation the two reactions (e) and (g) are possible. The corresponding change in the Gibbs free energy is given by

$$
\begin{aligned}
&4Fe + CO \underset{b}{\overset{f}{\rightleftarrows}} FeO + Fe_3C, \\
&\Delta G_0 = \text{Interpolation}[\ \{\{300,-88252\},\{400,-74245\},\{500,-61037\},\{600,-48353\},\\
&\{700,-35862\},\{800,-23376\},\{900,-10711\},\{1000,2359\},\{1100,16071\},\\
&\{1200,30199\},\{1300,44624\},\{1400,58962\},\{1500,73233\}\},\text{InterpolationOrder->1}](a) \\
&5Fe + CO_2 \underset{b}{\overset{f}{\rightleftarrows}} 2FeO + Fe_3C, \\
&\Delta G_0 = \text{Interpolation}[\{\{300,-76819\},\{400,-64475\},\{500,-53256\},\{600,-42751\},\\
&\{700,-32541\},\{800,-22375\},\{900,-12010\},\{1000,-1162\},\{1100,10473\},\\
&\{1200,22613\},\{1300,35110\}\},\text{InterpolationOrder->1}],(b)
\end{aligned}
\qquad (3.22)
$$

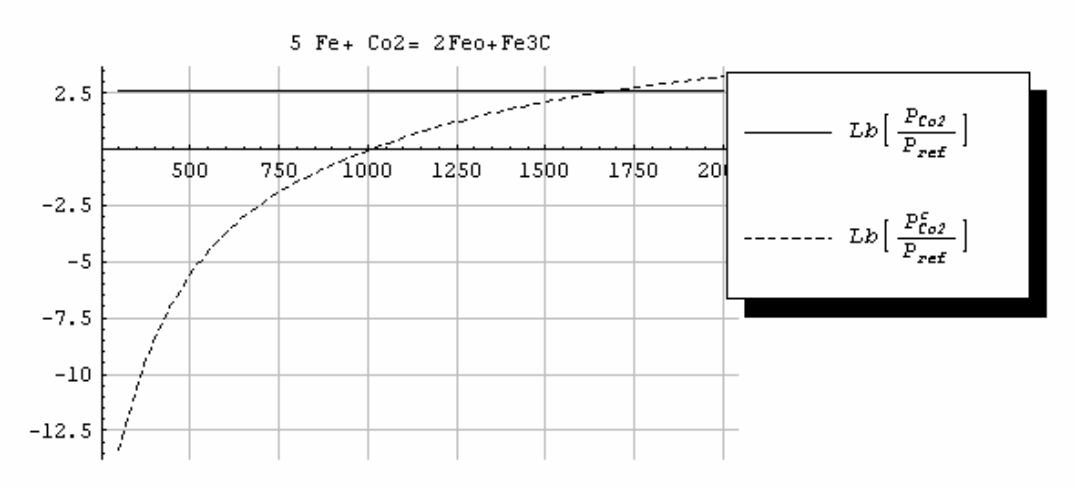

Figure 3.6: The Briggs logarithm of the relative pressure as a function of temperature T in Kelvin.

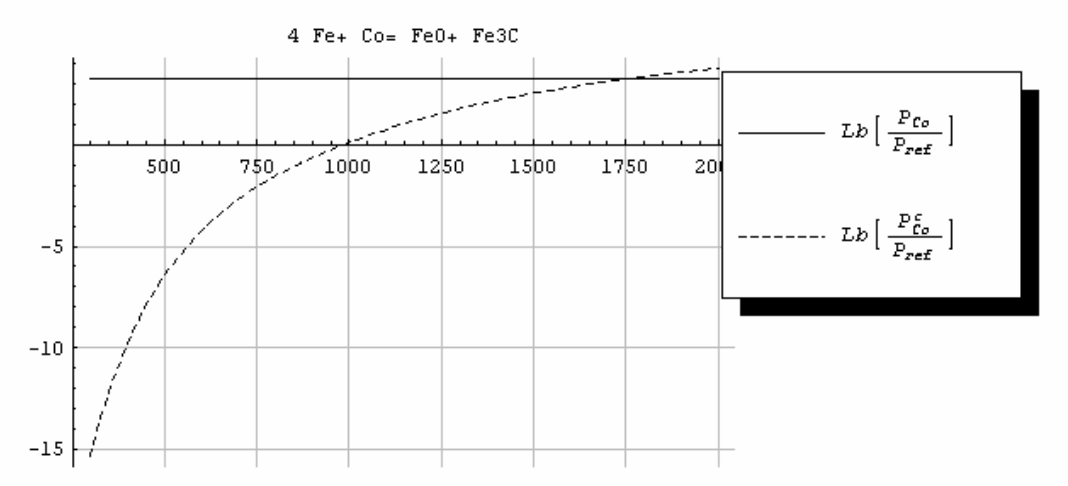

Equation (3.22b) is used. $P_{CO_2} = 3.88\,10^7\,Pa$.

Figure 3.7: The Briggs logarithm of the relative pressure as a function of temperature T in Kelvin. Equation (3.22b) is used. $P_{CO} = 1.910^8\,Pa$.

Figure 3.6 and Figure 3.7 clearly show that the reactions will go forward. The reactions are clearly exothermic with significant heat output for temperatures below 1500 K.

Summarizing, we believe that the three most important reactions concerning oxidation and carburisation are given as

$$
\begin{aligned}
&2Fe + O_2 \underset{b}{\overset{f}{\rightleftarrows}} 2FeO, (TGA-only)\\
&Fe + H_2O \underset{b}{\overset{f}{\rightleftarrows}} FeO + H_2,\\
&4Fe + CO \underset{b}{\overset{f}{\rightleftarrows}} FeO + Fe_3C,\\
&5Fe + CO_2 \underset{b}{\overset{f}{\rightleftarrows}} 2FeO + Fe_3C,
\end{aligned}
\qquad (3.23)
$$

We find that carbide is not the most thermodynamically stable reaction product.

4 THE OXYGEN PRESSURE

The oxygen pressure is of importance since oxides can not be reaction products unless the concentration of oxygen is above a certain limit that depends on the temperature. A question is whether the full thermodynamic calculations of the reaction products give the actual oxygen pressure during a shot. It is common knowledge that thermodynamic calculations, which use equilibrium assumptions, tend to overestimate the actual maximum pressure in a gun barrel during a shot. Thus an equilibrium assumption can be questioned. For this reason we will perform a quite different calculation. We calculate the different oxygen pressures and activities by studying the equilibrium reactions

$$\left\{\begin{array}{l} 2CO_2 \underset{b}{\overset{f}{\rightleftarrows}} 2CO + O_2, \Delta G_0 = 565650 - 173.88T \\ 2CO \underset{b}{\overset{f}{\rightleftarrows}} CO_2 + C, \Delta G_0(T) = -172670 + 175.94\,T \end{array}\right\} \qquad (4.1)$$
$$\left\{\begin{array}{l} 2H_2O \underset{b}{\overset{f}{\rightleftarrows}} 2H_2 + O_2, \Delta G_0 = 494420 - 112.8T \\ CO + H_2 \underset{b}{\overset{f}{\rightleftarrows}} H_2O + C, \Delta G_0 = -130279 + 160.38T \end{array}\right\}$$

The above reactions give a specific oxygen pressure and activity when the pressure of hydrogen, water vapour, carbon dioxide and carbon monoxide are given. From (4.1) it follows that during equilibrium

$$a): \left\{\begin{array}{l} \dfrac{p_{O_2}}{P_{ref}} = \dfrac{{P_{CO_2}}^2}{{P_{CO_2}}^2} Exp\left(-\Delta G_0 / (RT)\right), \Delta G_0 = 565650 - 173.88T \\ \dfrac{a_{C1}}{a_{ref}} = \dfrac{{P_{CO}}^2 P_{CO}}{P_{CO_2} P_{ref}} Exp\left(-\Delta G_0(T)/(RT)\right), \Delta G_0(T) = -172670 + 175.94\,T \end{array}\right. \qquad (4.2)$$
$$b): \left\{\begin{array}{l} \dfrac{p_{O_2}}{P_{ref}} = \dfrac{{P_{H_2O}}^2}{{P_{H_2}}^2} Exp\left(-\Delta G_0 / (RT)\right), \Delta G_0 = 494420 - 112.8T \\ \dfrac{a_{C1}}{a_{ref}} = \dfrac{P_{H_2} P_{CO}}{P_{H_2O} P_{ref}} = Exp\left(-\Delta G_0(T)/(RT)\right), \Delta G_0(T) = -130279 + 160.38T \end{array}\right.$$

Thus it follows from equation (4.2) and equation (3.13)

$$\left(\frac{a_{C1}}{a_{ref}}\right)/\left(\frac{p_{O_2}}{P_{ref}}\right)^{3/2} = \frac{{P_{CO}}^5}{{P_{CO_2}}^4 P_{ref}} Exp\left(-\Delta G_0(T)/(RT)\right), \Delta G_0(T) = -1021773 + 436.77\,T, (A)$$

$$\left(\frac{a_{C1}}{a_{ref}}\right)/\left(\frac{p_{O_2}}{P_{ref}}\right)^{3/2} = \frac{P_{CO}{P_{H_2}}^4}{{P_{H_2O}}^4 P_{ref}} Exp\left(-\Delta G_0/\left(RT\right)\right)\Big), \Delta G_0 = -871909 - 275.58T, (B) \qquad (4.3)$$

$$\left(\frac{a_C^{c'}}{a_{ref}}\right)/\left(\frac{p_{O_2}}{P_{ref}}\right)^{3/2} = Exp\left(\Delta G_0(T)/(RT)\right), \Delta G_0(T) = 818056 - 224.37\,T, (C)$$

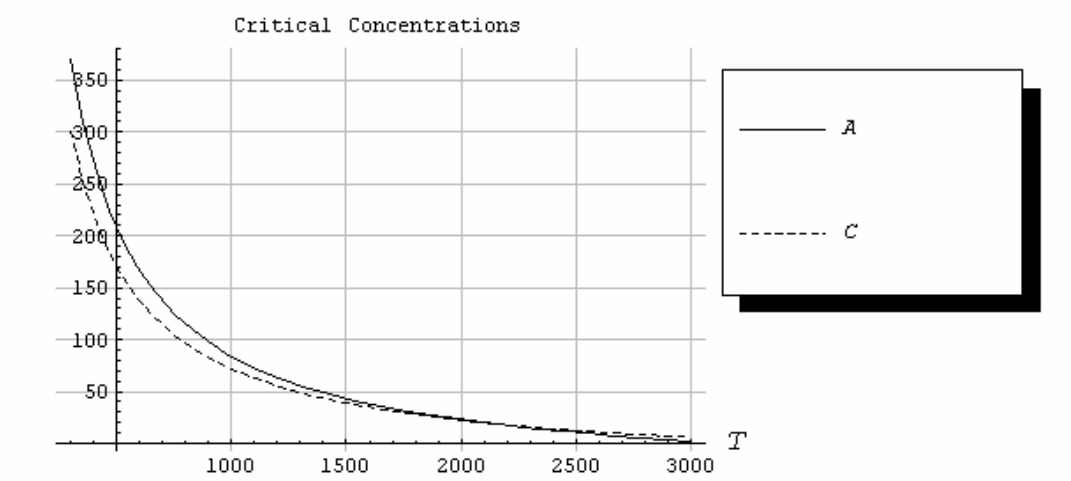

Figure 4.1: The dependence of $\left(\frac{a_{C1}}{a_{ref}}\right)/\left(\frac{p_{O_2}}{P_{ref}}\right)^{3/2}$ = A, and $\left(\frac{a_C^{c'}}{a_{ref}}\right)/\left(\frac{p_{O_2}}{P_{ref}}\right)^{3/2}$ = C *as a function of temperature T in Kelvin. Equation (4.3) is used.* $P_{CO} = 1.910^8\,Pa$, $P_{CO_2} = 3.88\,10^7\,Pa$

We find that for temperatures below 1800 K the iron carbide is the most stable reaction product, and not the iron oxide. This result is in disagreement with the result in section 3, which shows that iron oxide is the most stable reaction product. But in section 3 the oxygen pressure was calculated by

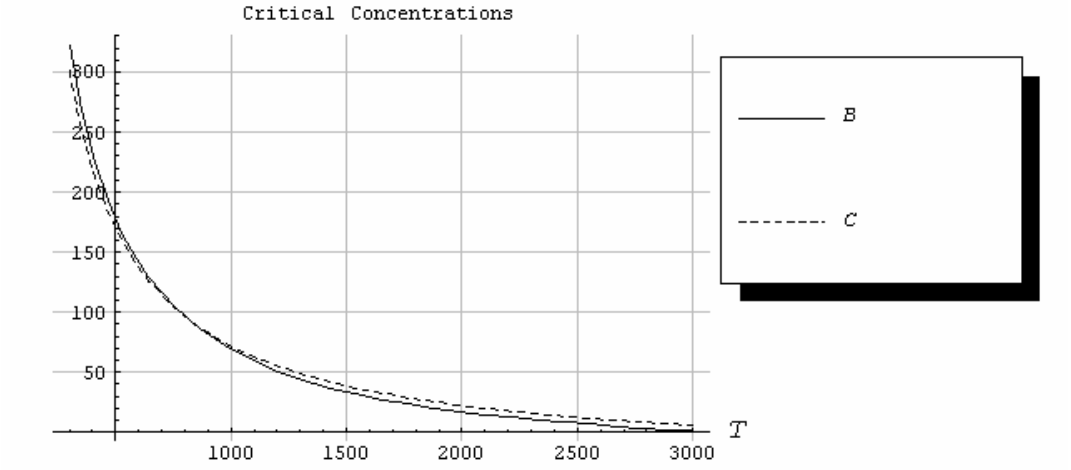

assuming thermodynamic equilibrium during a shot.

Figure 4.1: The dependence of $\left(\frac{a_{C1}}{a_{ref}}\right)/\left(\frac{p_{O_2}}{P_{ref}}\right)^{3/2}$ = B, and $\left(\frac{a_C^{c'}}{a_{ref}}\right)/\left(\frac{p_{O_2}}{P_{ref}}\right)^{3/2}$ = C *as a function of temperature T in Kelvin. Equation (4.3) is used.*
$P_{CO} = 1.910^8\,Pa$, $P_{CO_2} = 3.88\,10^7\,Pa$, $P_{H_2O} = 9.48\,10^7\,Pa$, $P_{H_2} = 5.6\,10^7\,Pa$.

In Figure 4.1 we use the reaction in equation (4.1b) to calculate the oxygen pressure. Now we find that for temperatures below 800 K the reaction product is iron carbide, i.e. iron carbide is the thermodynamic most stable reaction product.

We have thus reached the following conclusions. Wüstite and cementite can be reaction products during a shot. The most stable reaction product is wüstite if the full thermodynamic equilibrium situation is assumed during a shot. For situations where the full thermodynamic equilibrium is not advanced, the most stable reaction product depends on the actual reaction that determines the oxygen pressure and the carbon activity during a shot. If the reaction in (4.1) is assumed, we find that iron carbide (cementite) is the most thermodynamically stable product for temperatures below 1800 K. If the reaction in (4.1b) is assumed, we find that for temperatures below 800 K the iron carbide is the most stable reaction product, while iron oxide (wüstite) should be the most stable one for temperatures above 800 K.

5 THERMOGRAVIMETRIC RESULTS

In order to analyse the oxidation and carburisation behaviour more closely, different gases were used in a thermogravimetric analyzer (TGA) shown in Figure 5.1. The experimental recording was the weight of the cylindrical specimen which was cut from the gun barrel. The gas flow during experiments was always ~100 mL/min through the furnace under atmospheric pressure.

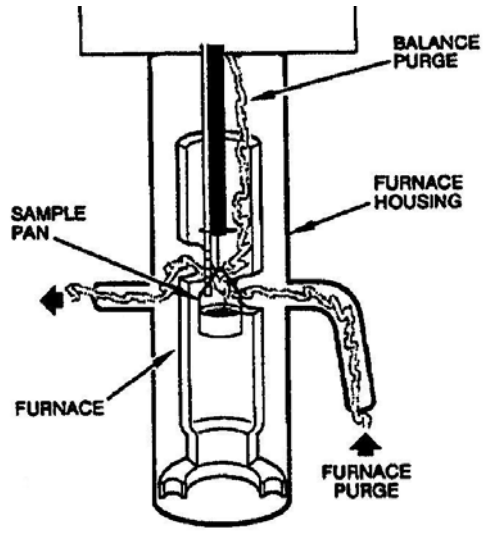

Figure 5.1: The TGA instrument.

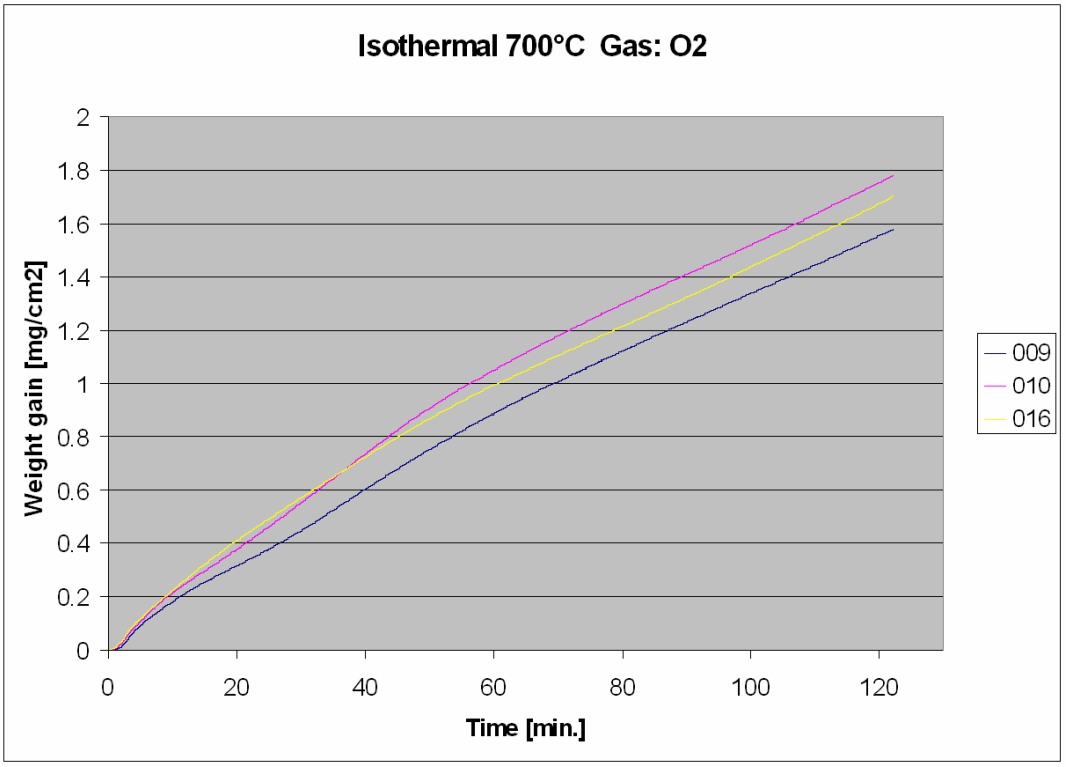

Figure 5.2: The weight gain as a function of time for 700°C using oxygen. Three experiments.

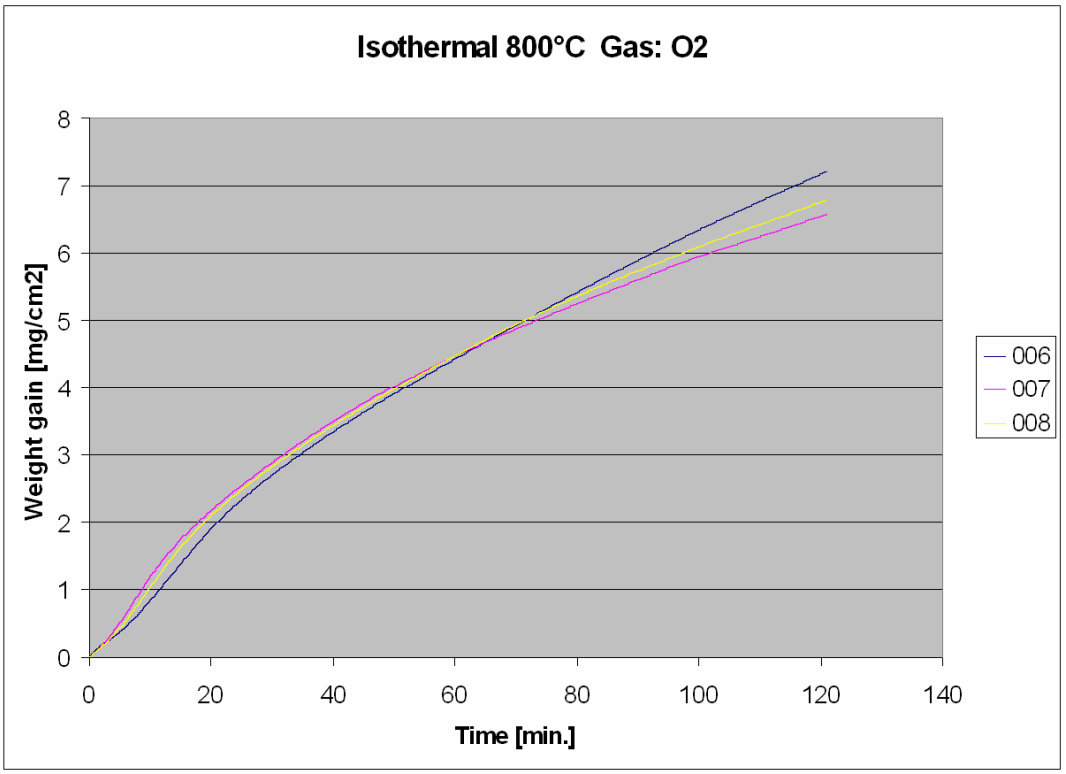

Figure 5.3: The weight gain as a function of time for 800°C in oxygen. Three experiments.

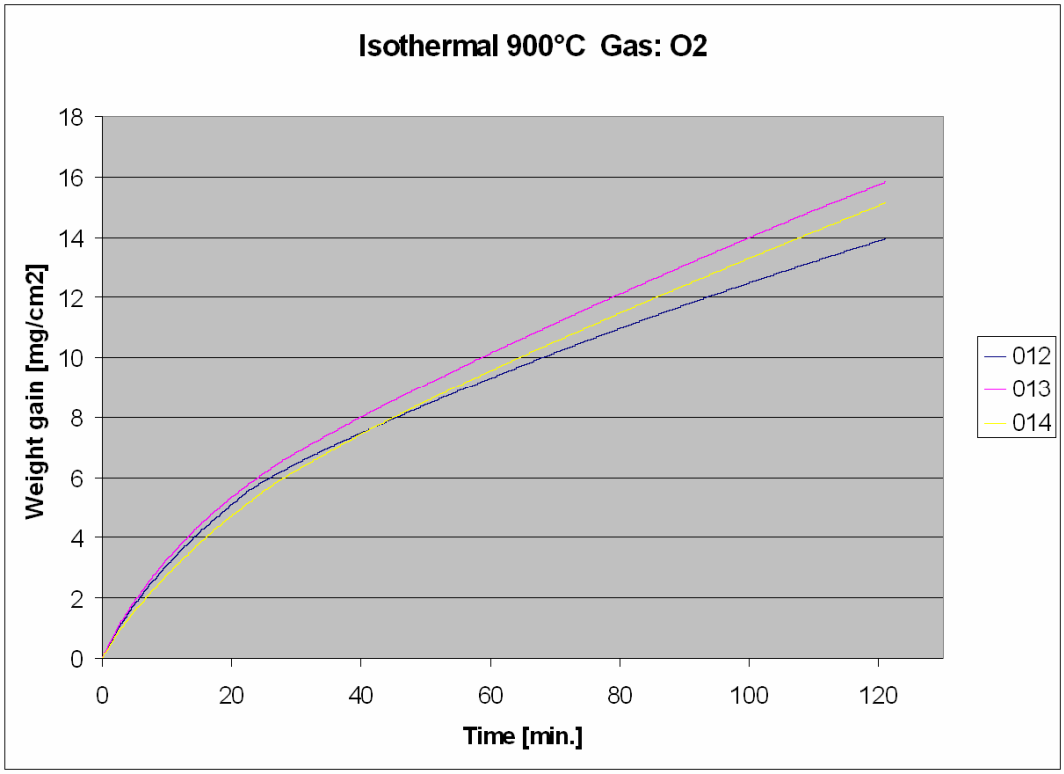

Figure 5.4: The weight gain as a function of time for 900°C in oxygen. Three experiments.

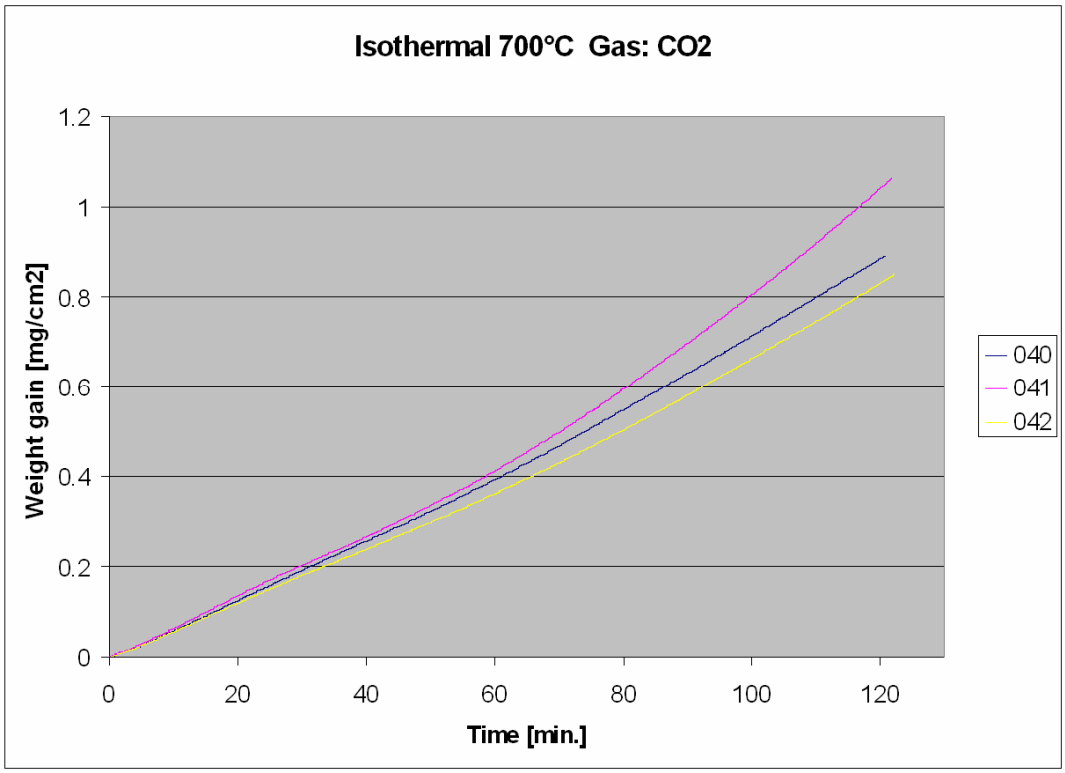

Figure 5.5: The weight gain as a function of time for 700°C in carbon dioxide. Three experiments.

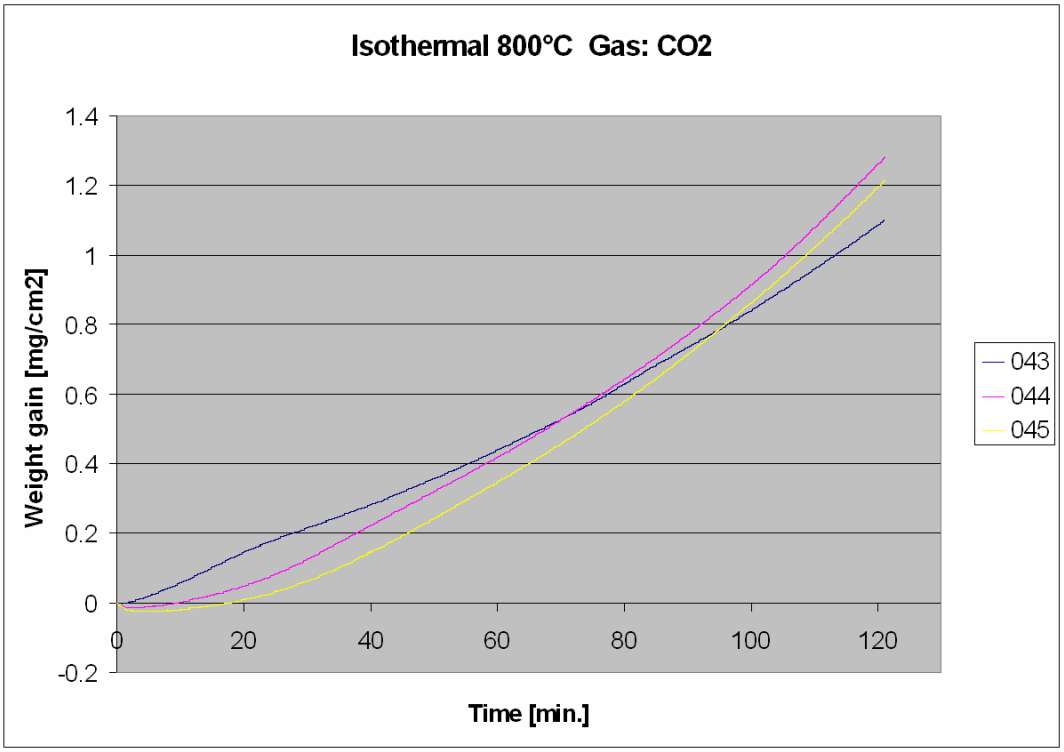

Figure 5.6: The weight gain as a function of time for 800°C in carbon dioxide.

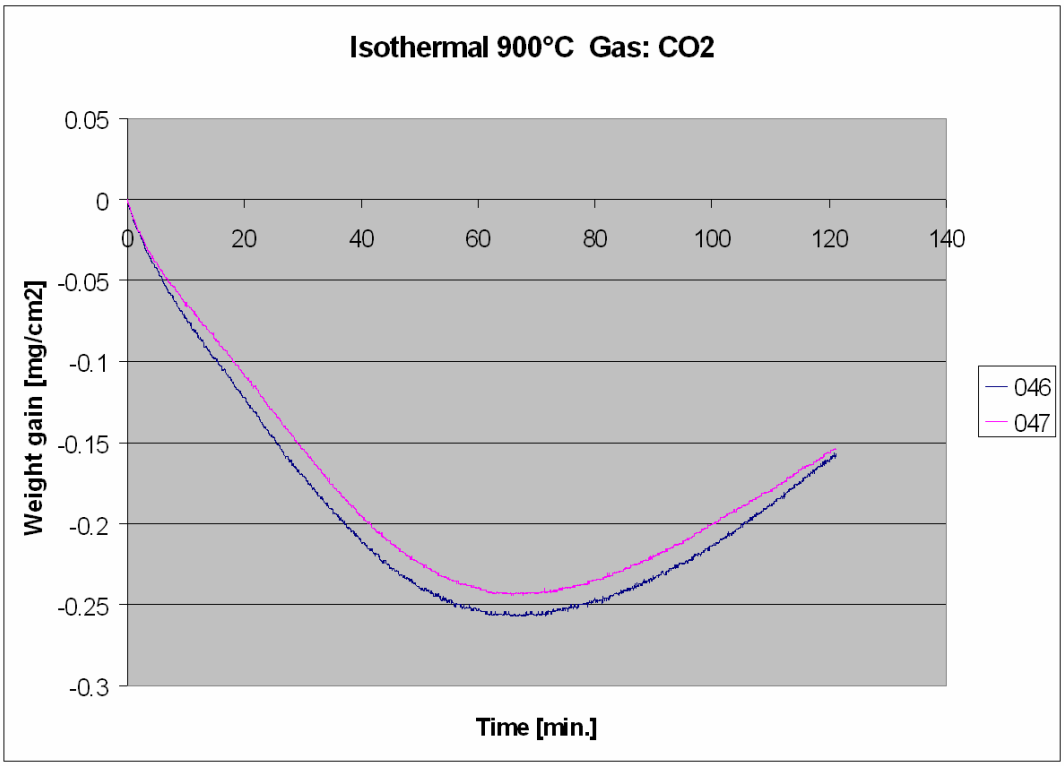

Figure 5.7: The weight gain as a function of time for 900°C in carbon dioxide.

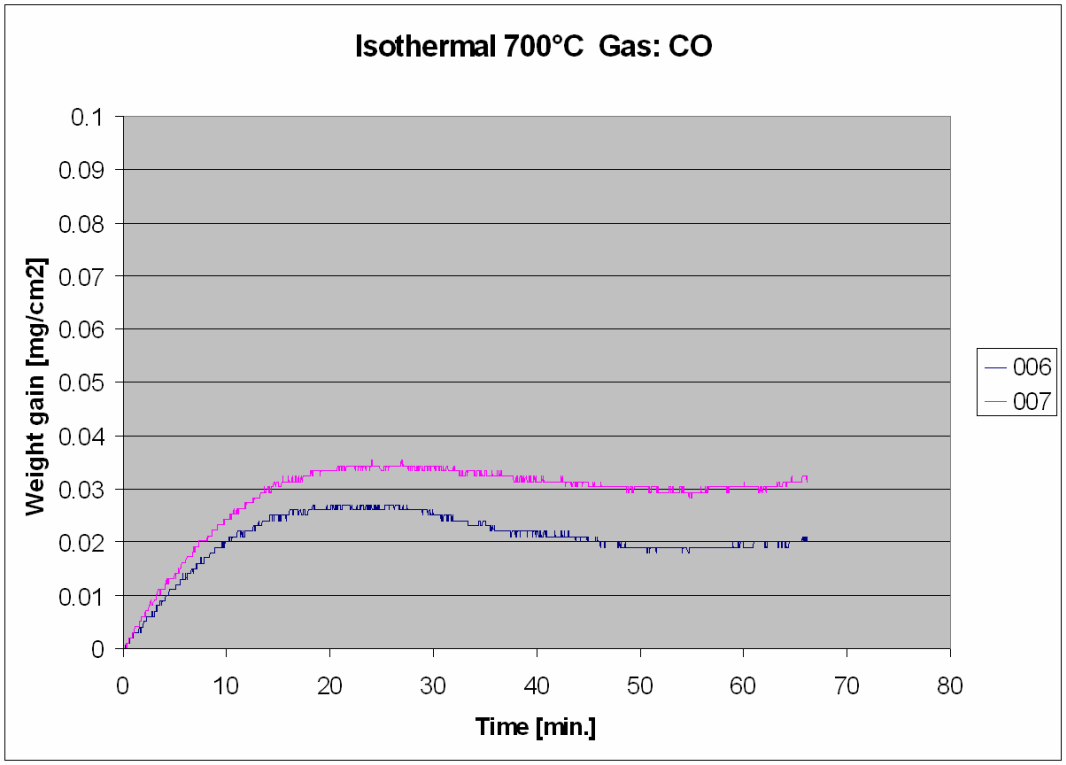

Figure 5.8: The weight gain as a function of time for 700°C in carbon monoxide.

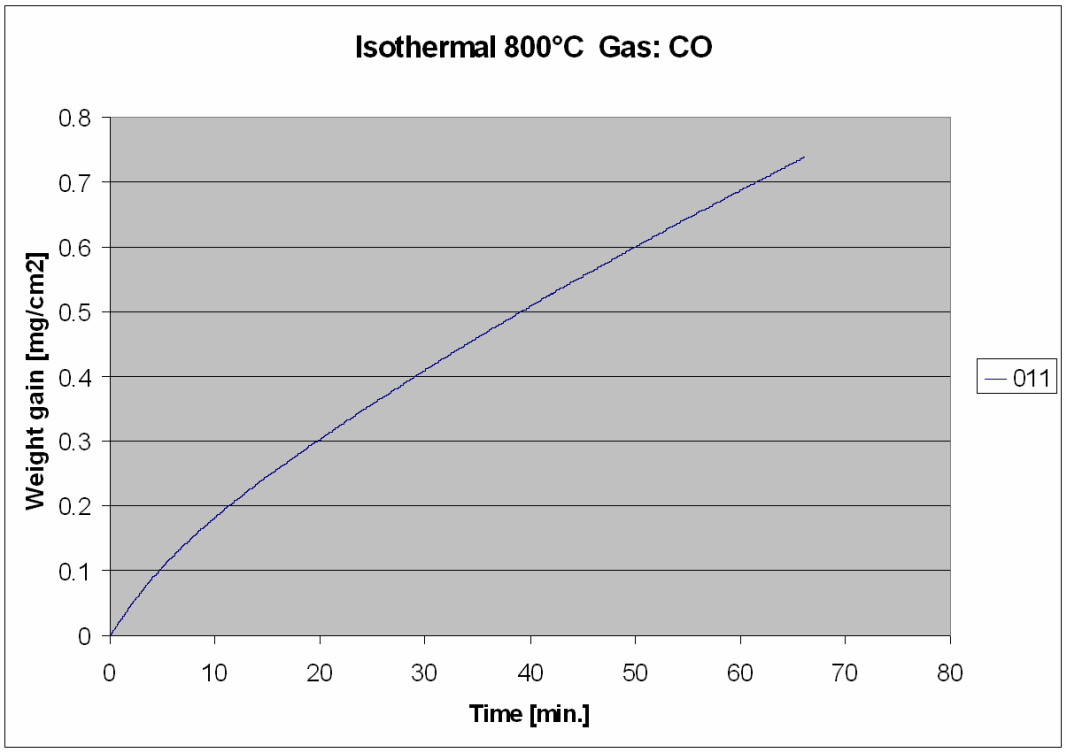

Figure 5.9: The weight gain as a function of time for 800°C in carbon monoxide.

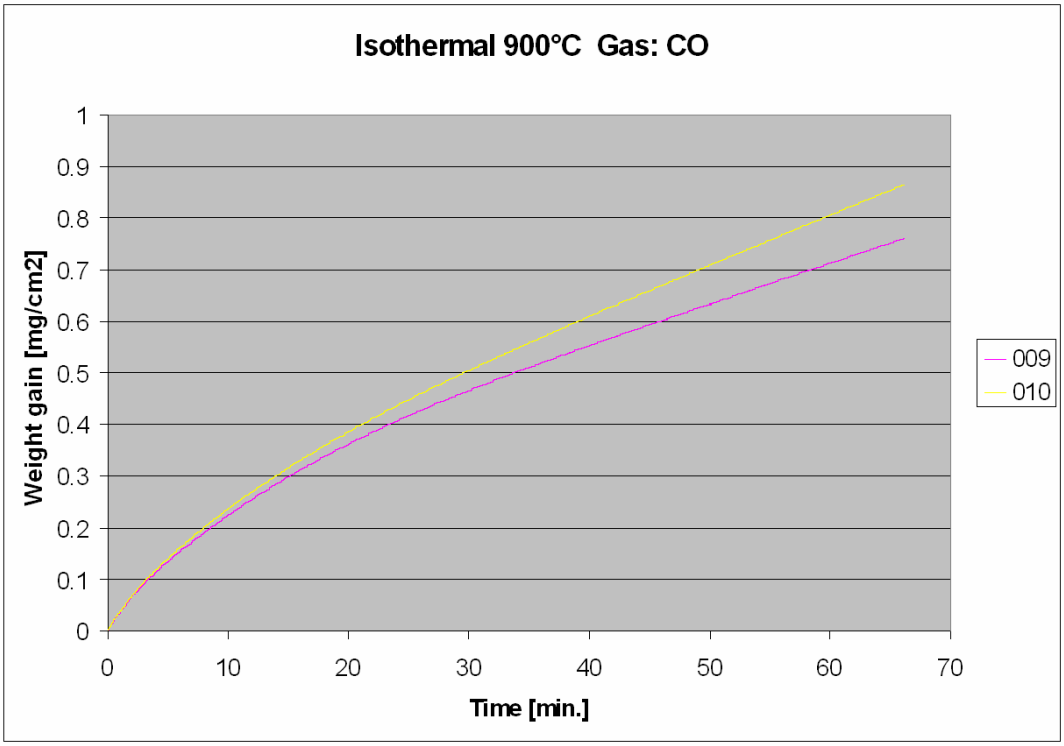

Figure 5.10: The weight gain as a function of time for 900°C in carbon monoxide.

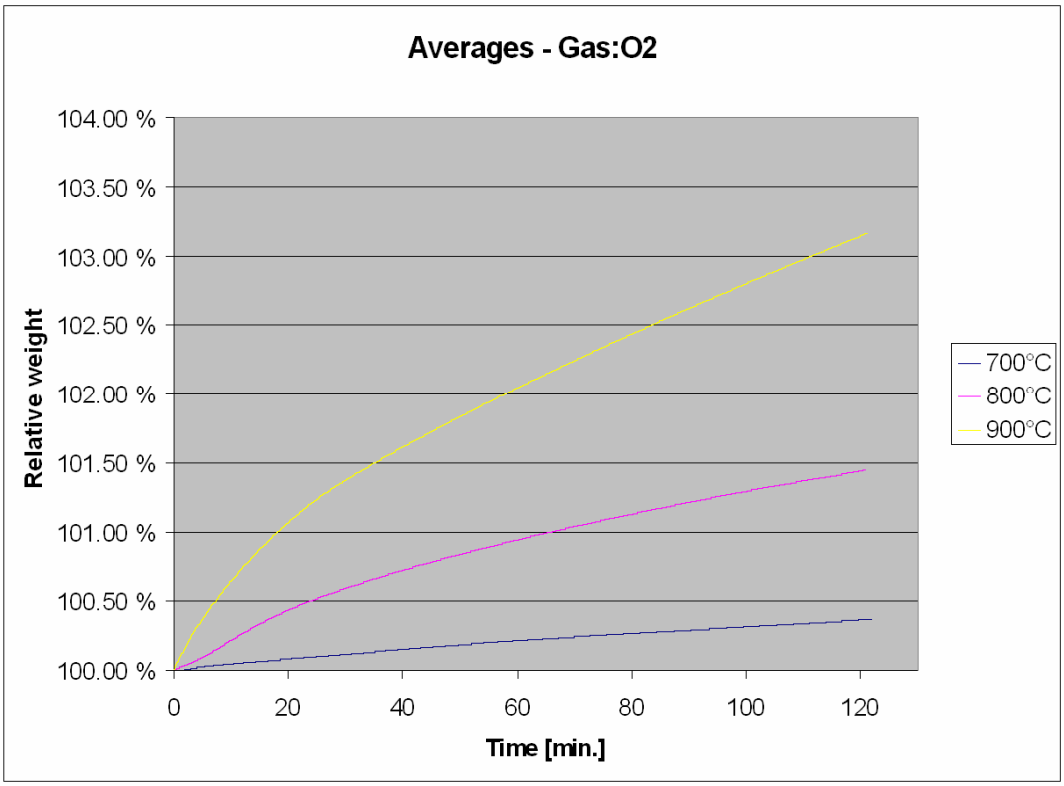

Figure 5.11: The average weight gain as a function of time for 700°C-900°C in oxygen.

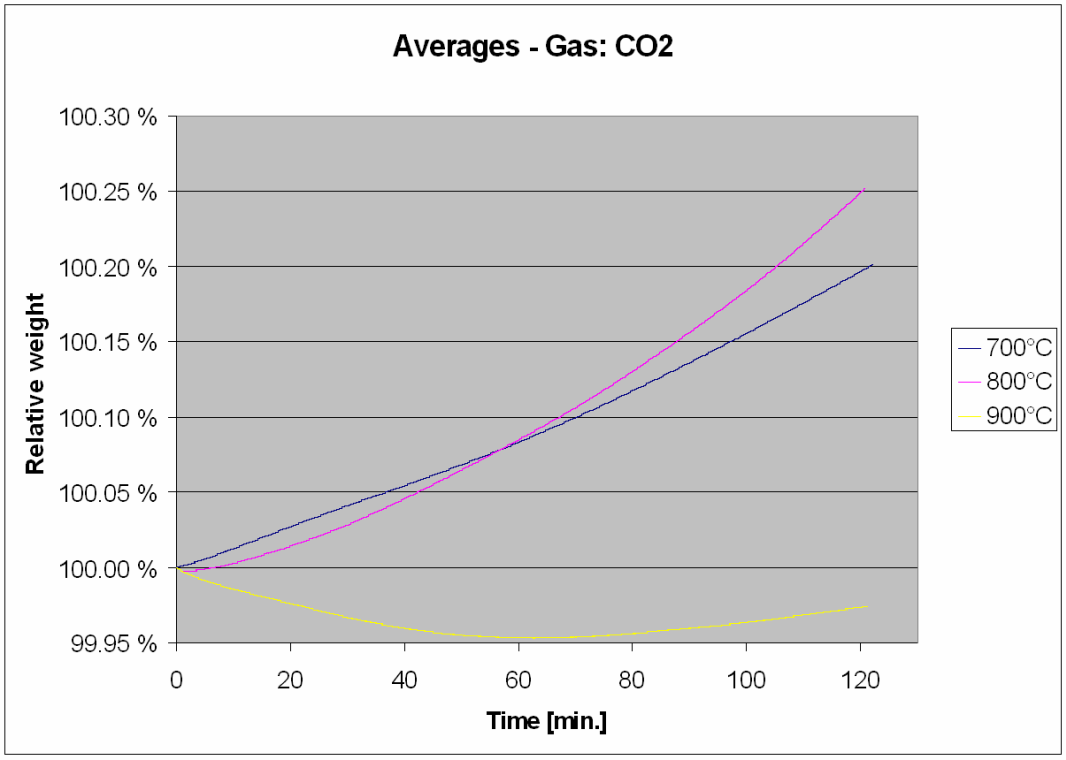

Figure 5.12: The average weight gain as a function of time for 700°C-900°C in carbon dioxide.

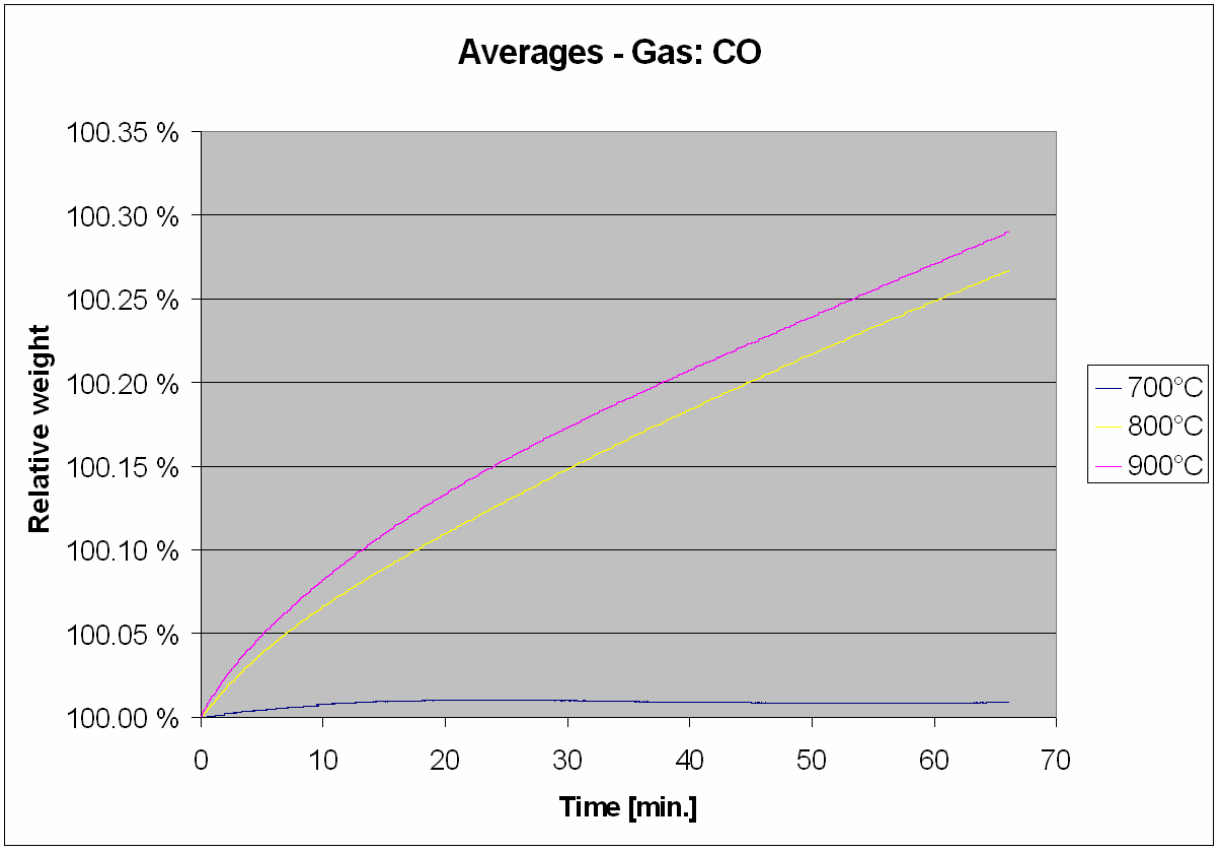

Figure 5.13: The average weight gain as a function of time for 700°C-900°C in carbon monoxide.

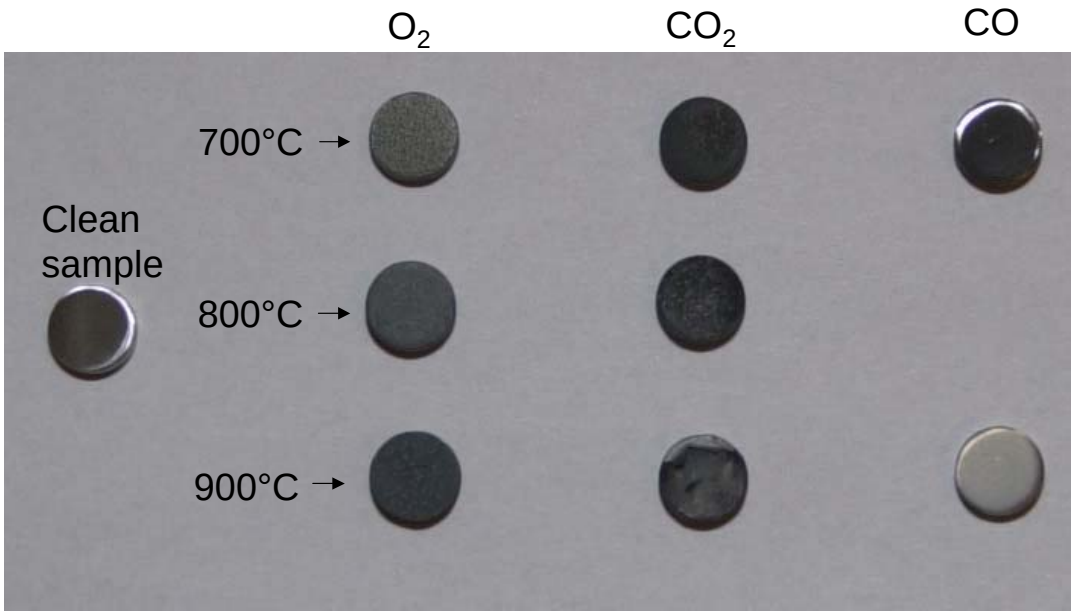

Figure 5.14: The different pellets after being exposed to different gases.

For the oxygen gas Figure 5.11 shows that the weight gain becomes larger for larger temperatures. For the carbon dioxide gas the weight gain is much smaller than for oxygen gas, and also the behaviour is more complex. For temperatures as high as 900°C the weight gain is negative. We believe that figure 3.6 could explain this phenomenon. When changing to a carbon dioxide concentration of 1 bar the horizontal line in figure 3.6 becomes the x axis. Thus a crossing point of the two curves will be at around 1000 K. For temperatures above 1000 K the critical carbon dioxide concentration is above the carbon dioxide pressure of 1 bar and the reaction will not take place.

Probably the reaction in figure 3.4 is the most natural if the fraction of carbon dioxide to carbon monoxide is high enough. We do not know this fraction in our TGA gas.

Further studies are necessary to explain why the carbon dioxide gas gives weight gain for temperatures at least as high as 1100 K. One explanation is that the critical pressure curve in figure 3.6 should have been shifted somewhat to the right, thereby giving a crossing point at 1100 K instead of 1000 K. We have compared our theoretical results with an alternative thermodynamic program and found such a shift.

For the carbon monoxide gas the weight gain is small. It seems that higher temperatures give higher weight gain. We believe that figure 3.7 could explain some of our results. The horizontal line is changed to the x-axis when using the TGA analysis. Thus for temperatures below 1000 K cementite and wüstite should be possible to create. But this conclusion is not in close agreement with our experimental results since we see a weight gain for 1200 K. To study this more closely we have performed hardness measurements of the specimens after the heat treatment in the TGA. We have found that for temperatures at 900°C with CO the hardness is larger than for the O_2, CO_2 and Ar gases. Our suggestion is thus that the reaction taking place during the thermogravimetric analysis for carbon monoxide is $Fe + CO \underset{b}{\overset{f}{\rightleftharpoons}} FeO + C$. The carbon diffuses further into the steel. To achieve the forward reaction the carbon activity must be low enough.

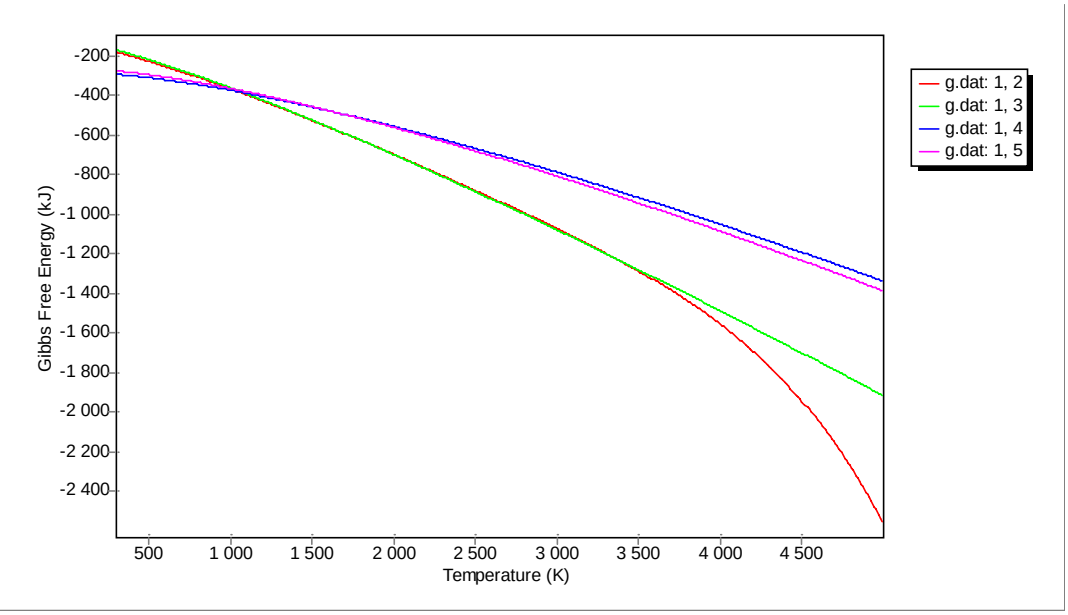

Figure 5.15: The Gibbs Free energy of the reactants and the products for the reaction $Fe + CO \underset{b}{\overset{f}{\rightleftharpoons}} FeO + C$. *g.dat: 1,4 and g.dat 1,5 gives the reaction products when assuming solid carbon and solid or liquid FeO respectively. g.dat1,2 and g.dat1,3 gives the reactants when assuming solid or liquid Fe respectively.*

Figure 5.15 shows the Gibbs free energies when assuming the activity of carbon to be one (solid) and assuming 1 bar. The figure shows that the reaction will advance forward for temperatures below 1100 K. See the next section for further studies.

6 FURTHER TGA STUDIES WITH HARDNESS MEASUREMENTS

The behaviour of the steel specimen taken from a gun barrel (Browning M2 machine gun) was examined during different conditions. We used the TGA for 2.5 minutes, 10 minutes, 1 and 2 hours. Two different cylindrical specimens with different thickness were used. Also different gases were used. The specimens were cooled in the furnace without any control of the cooling rate. The cooling time is around 46 minutes each time (from 900°C to 50°C. See appendix A). Some of the specimens were quenched in water.

The hardness was measured in the internal of the specimen after being embedded in epoxy. Figure 6.1 and figure 6.2 give the results. We found that the hardness changed to higher values for temperatures at 900°C. For temperatures at 700°C the hardness decreased slightly. For 900°C the hardness decreased for longer exposure times, although for specimens with 2 mm thickness the hardness seems to be nearly constant for any exposure time. The quenching gave the largest hardness for the specimens not run in CO gas.

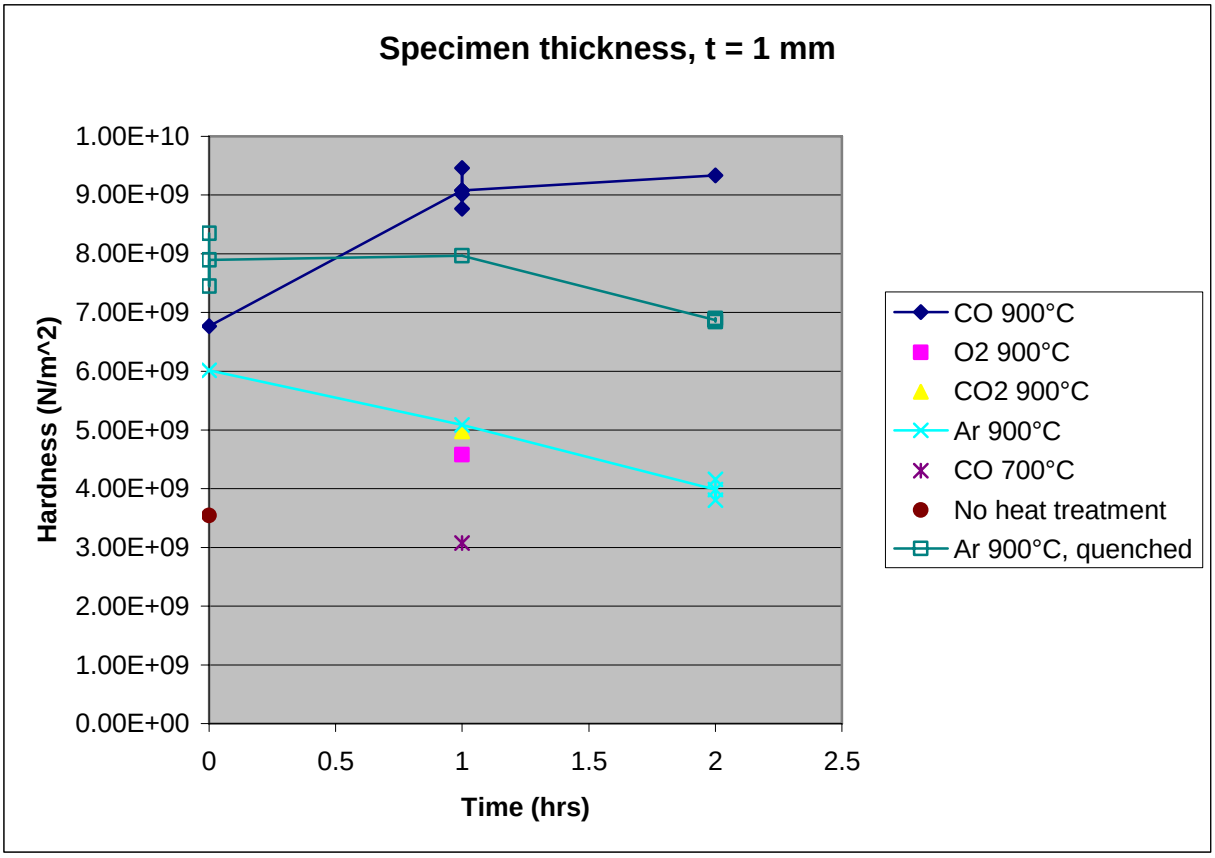

Figure 6.1: The hardness of steel specimens after heat treatment in TGA.

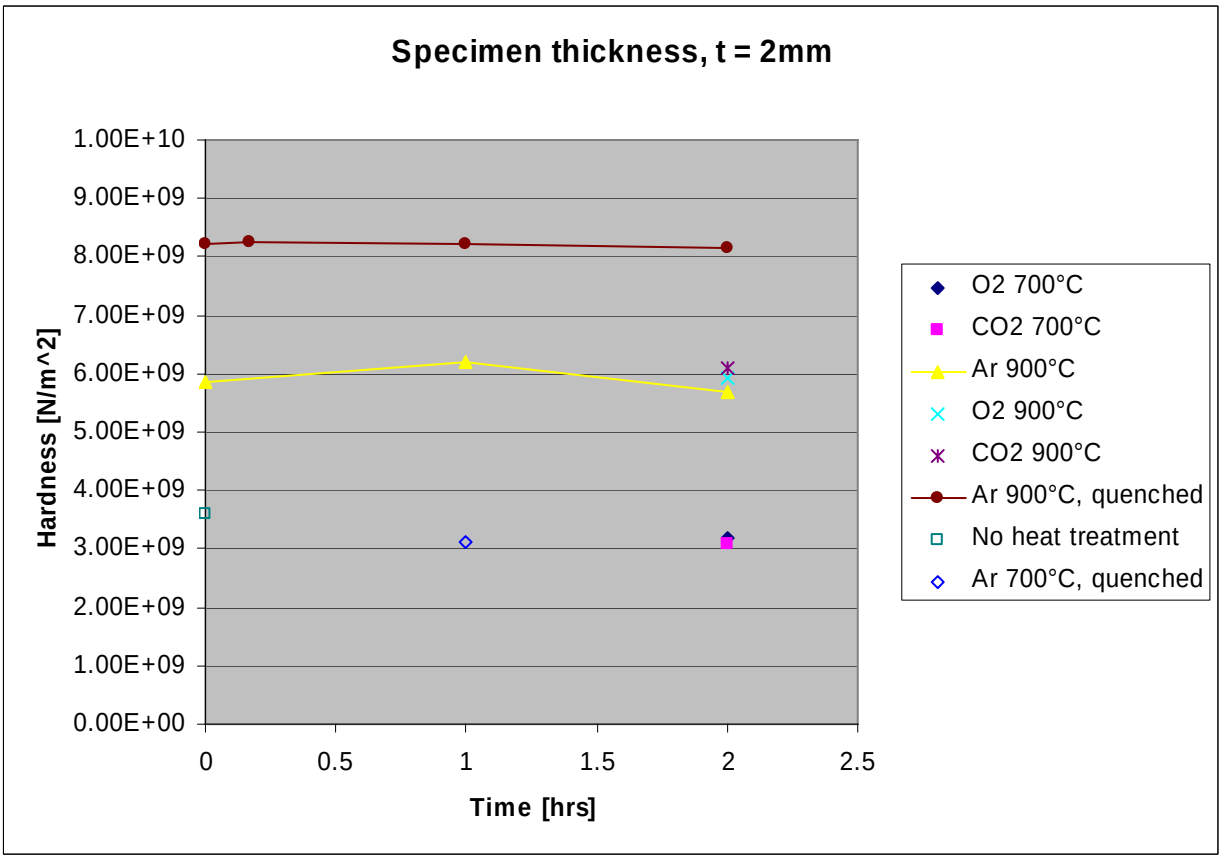

Figure 6.2: The hardness of steel specimens after heat treatment in TGA.

Our comments of the results are as follows: Our type of specimens cut from the gun barrel steel is a low alloy steel with 0.41 % carbon. Before our heat treatment the hardness test shows that we have only an insignificant amount of martensitic structure [1]. The structure is mainly ferrite and cementite (tempered martensite). The martensitic structure is a hard and brittle structure where dislocation motion is limited due to entrapped carbon atoms in the steel. To achieve martensite the steel (cementite/ ferrite) must first be heated up to a gamma structure (austenite). The phase change takes place at 800°C for our gun barrel steel [2]. Thereafter carbon atoms must have time to diffuse into the austenite structure. Thereafter the cooling rate must be high enough to "freeze" the carbon in a distorted body-centered cubic structure. Thus to reach a martensitic structure the temperature must be high enough, the heating time must be long enough and the cooling rate must be high enough. The martensite is not thermodynamically stable (metastable), so it will in the long run be transformed to ferrite and cementite. The literature shows that the low amounts of alloying elements in the gun barrel steel do not significantly change the hardness or the ductility of the steel compared to a plain carbon steel. But the smallest cooling rate to achieve 100 % martensite is significantly decreased compared to a plain carbon steel. Also the maximum amount of martensite in a structure will change with the fraction of alloying elements. In general the alloying elements increase the smallest heating time and decrease the smallest cooling rate to achieve 100 % martensite. The reason for the longer heating time and smaller cooling rate is that the alloying elements tend to stop the diffusion velocity of carbon in the steel structure.

The literature gives that for a 100 % martensitic structure the hardness becomes around 8 GPa (770 HV) when the carbon content is around 0.41 % as in our specimen. When using the CO_2, Ar or the O_2 we found values in our TGA analysis close to this for almost all data points when using quenching in water for heat treatments at 900°C. The 2 hours heating time with quenching gives another result. We notice that for the 1 mm thickness specimens the hardness decreases with the heating time when cooling in the furnace. We believe that this is due to carbon diffusing out of the steel specimen. We do not know why the results for the 2 mm thickness, which shows an almost constant hardness, is different from the result for the 1 mm. But one explanation could be that the carbon is not diffusing out of the steel specimen due to the lager thickness. In general we observe that the cooling time in the furnace of approximately 10 minutes (900°C → 300°C) is too high to give 100 % martensite.

The CO gas gives a different result. Due to experimental problems we could not quench the specimens in water when CO was used. The elevated hardness for the CO gas compared to the other gases, we believe, is caused by carbon diffusion into the steel from the carbon monoxide gas during the heat treatment. Thus effectively increasing the carbon fraction in the steel. The diffusion from the surface takes some time, and the results for the smallest heating time (around 2.5 minutes from 700°C to 900°C) clearly shows this since the hardness is not very different from the other gases.

The hardness for small heating times (around 2.5 minutes from 700°C to 900°C) using the CO gas or the other gases in the TGA is the same as the hardness of the heat affected zone of the lands of a gun barrel. We believe that the heating time for the lands of the gun barrel steel during a shot are too small to give significant heating, and also too small for carbon diffusion from the surface. The lands are strongly heated for only milliseconds only during a shot. Thus our conclusion is that the increased hardness of the lands is a significant martensitic development caused by the elevated temperature (above 800°C) and the fast cooling rate, and not by increased carbon fraction.

7 MORE OXIDATION STUDIES

Further oxidation studies were performed. Of special interest was the growth of the oxide layer. The figures below give the results from our oxidation study. For low temperatures (600°C) the oxide layer grows inward. The reason is that the outward flux of iron particles from the iron surface is small compared to the diffusion of oxygen into the steel. Thus the reaction zone is close to the surface. For higher temperatures (900°) the outward flux of iron particles is much larger and the reaction takes place above the surface. Thereby leading to outward growth. To further check the phenomenon we have used a platinum sample situated on the steel surface. Observe that the platinum sample is situated in layer no. 2 as counted from the steel surface. Thus layer no. 1 is growing inward while layer no. 2 and 3 are growing outward. A crack is developed between layer no. 1 and layer no. 2. We believe that the crack has been made during the cooling process of the sample. At 600°C there is a much smaller layer (figure 7.2). This layer is inward growing and is probably FeO. Figure 7.3 shows typical thicknesses of the layers at 900°C. A large crack between the steel and layer no. 1 is seen. Layer no. 1 has been growing inward.

An EDS (Energy dispersive x-ray spectrometry) analysis has also been used to check the types of atoms in the different oxide layer. Typically alloying elements in the steel are found in the inward growing layer which we believe is mainly FeO. The outward growing layers are probably Fe_3O_4 and Fe_2O_3. Figure 7.4 shows a close-up of the different layers and tells where the EDS analysis has been performed. Figures 7.5 to figure 7.8 gives the results from the EDS analysis. Observe that the alloying elements of the steel are found in the inward growing layer only. Figure 7.9 and figure 7.10 show the results for the CO_2 and the CO respectively.

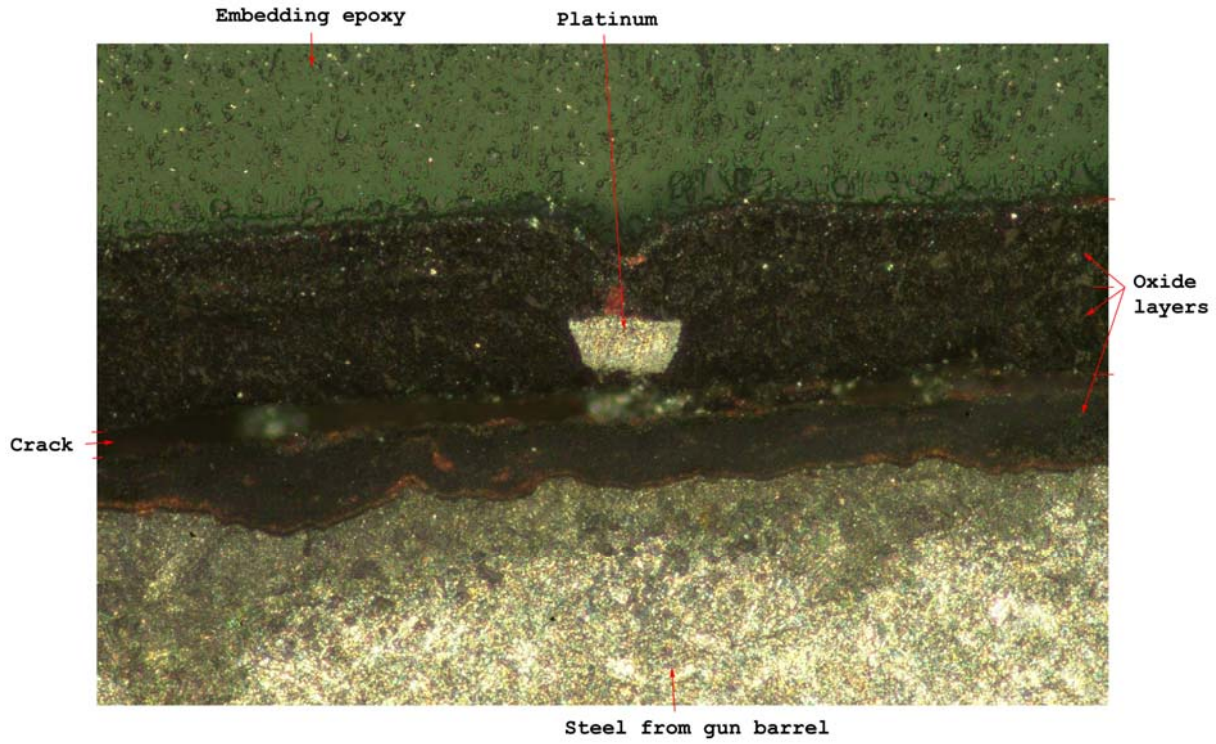

Figure 7.1: O_2 at 900°C. (Optical microscope)

Figure 7.2: O_2 at 600°C. (Optical microscope)

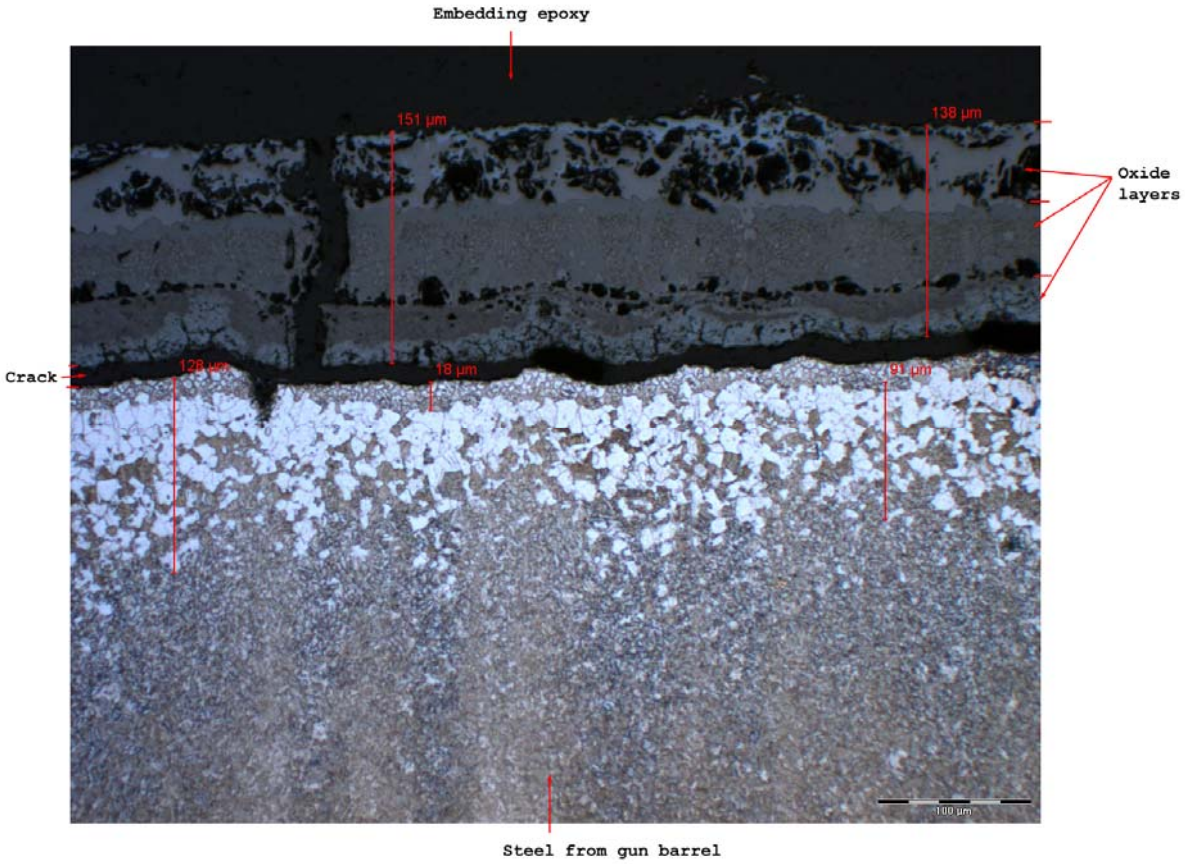

Figure 7.3: *O_2 at 900°C. (Optical microscope)*

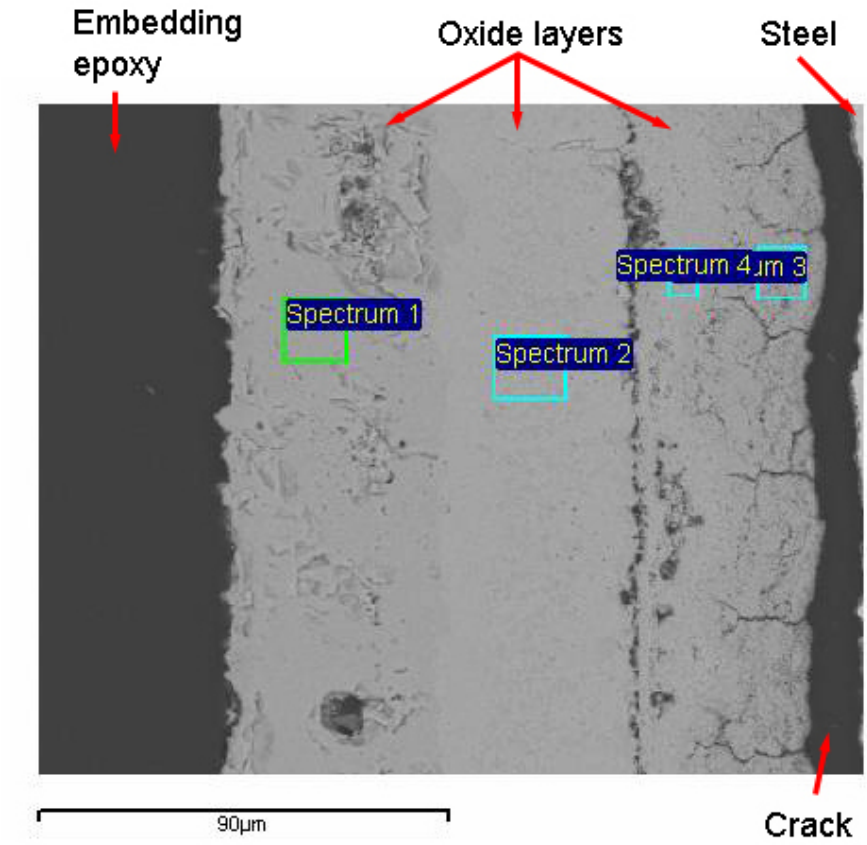

Figure 7.4: Zones for EDS-analysis of oxide layers.

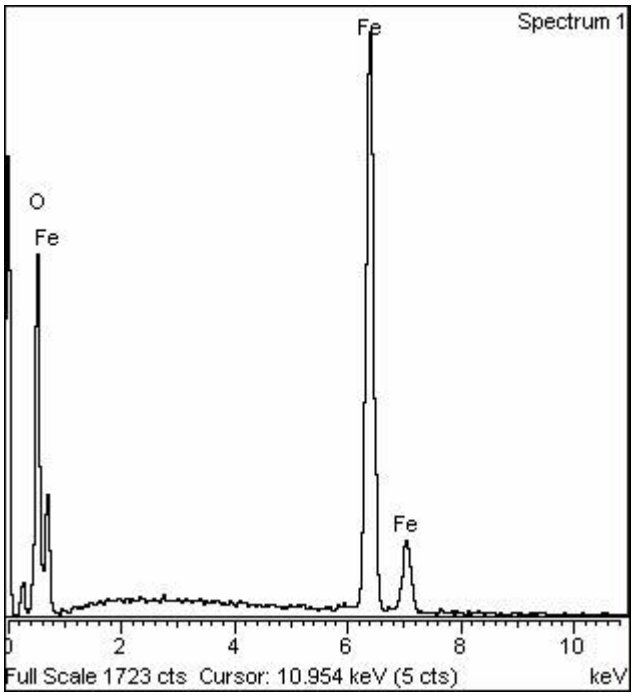

Figure 7.5: Spectrum 1 in figure 7.4.

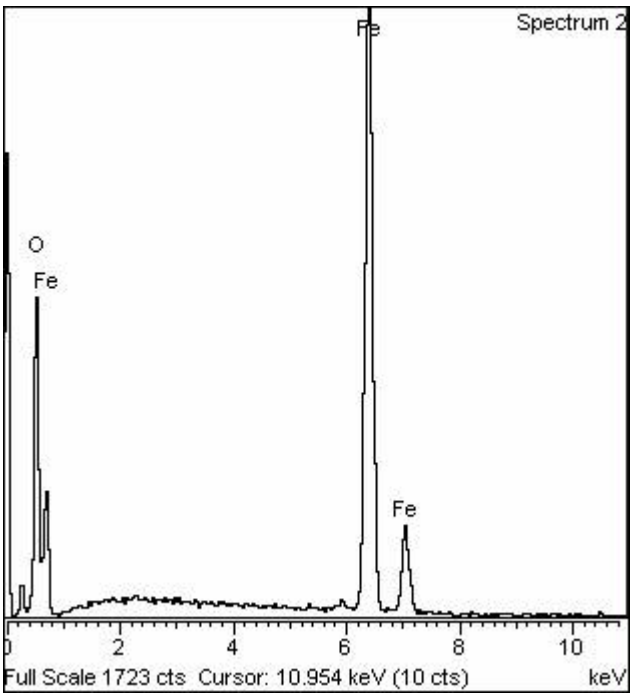

Figure 7.6: Spectrum 2 in figure 7.4.

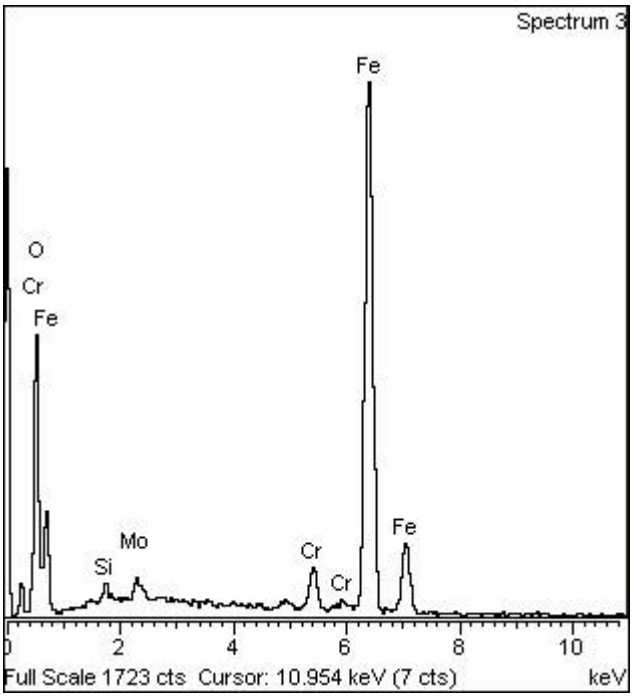

Figure 7.7: Spectrum 3 in figure 7.4.

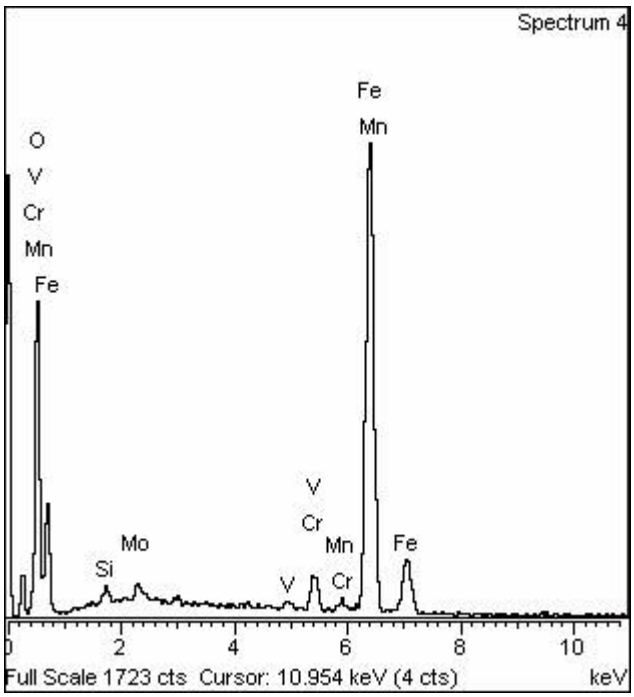

Figure 7.8: Spectrum 4 in figure 7.4.

Figure 7.9: CO_2 at 700°C. (Optical microscope)

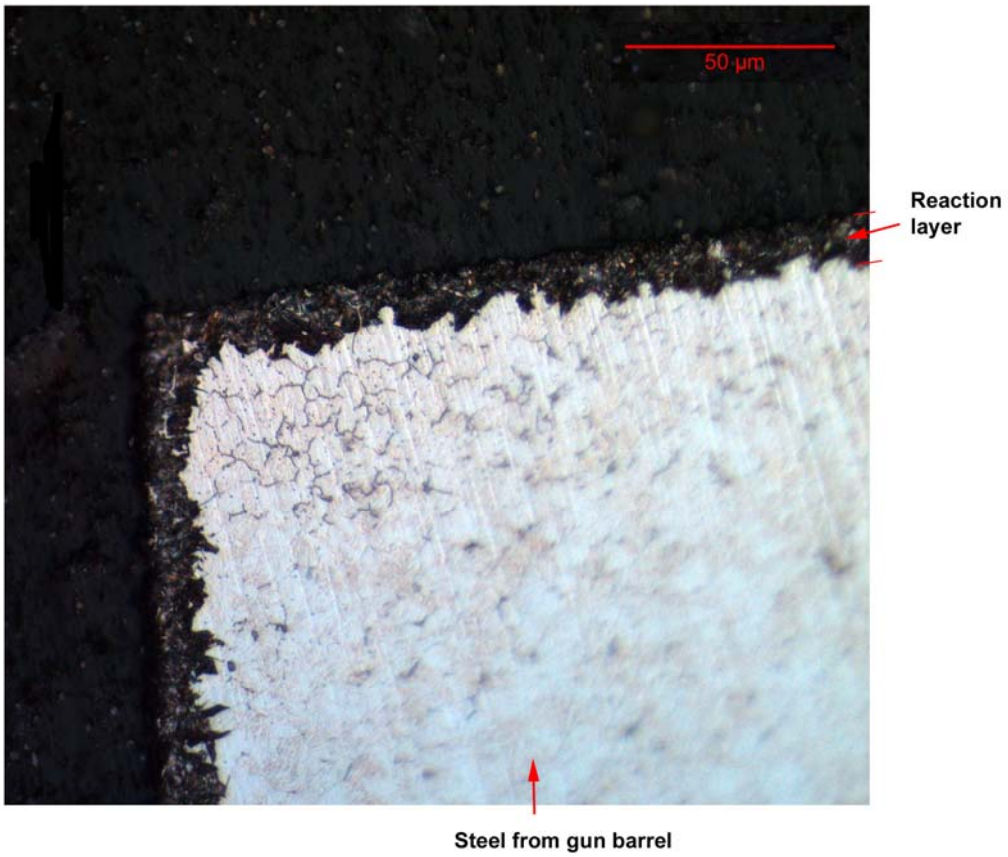

Figure 7.10: CO at 900°C. (Optical microscope)

8 CONCLUSION/DISCUSSION

In this report a theoretical and experimental study of some basic gun barrel erosion mechanisms has been carried out. The theoretical analysis of the reaction mechanisms is based on the minimalization of Gibbs free energy. Oxygen, carbon dioxide, carbon monoxide and argon are used for experimental study in a thermogravimetric analyzer. The thermogravimetric experiments are compared with theoretical results and some discrepancies are found. Hypothesises are put forward also based on hardness measurements of heat affected steel specimens cut from the gun barrel.

Indeed, we find that the reaction mechanisms are quite complex. One important conclusion related to the wear of gun barrels is that the increased hardness of the heat affected zone on the lands of gun barrels is not caused by carbon diffusion from deposits on the surface from the gun barrel gases. The increased hardness of the heat affected zone together with our experimental study in this report suggests that a martensitic structure is established purely due to temperature changes during a shot. The hardness of 6 GPa on the lands of gun barrels suggests that the cooling rate during a shot is not large enough to reach 100 % martensite, corresponding to a value of 8 GPa for our carbon steel of 0.41 % carbon.

In general we believe that some basic insight into the general problem of gun barrel wear has been achieved through the theoretical and experimental study in this report.

References

[1] A. Almar-Næss, Metalliske materialer, Tapir, akademisk forlag, fjerde utgave, Trondheim 2003, ISBN82-519-1786-7, page 243
[2] A. Almar-Næss, Metalliske materialer, Tapir, akademisk forlag, fjerde utgave, Trondheim 2003, ISBN82-519-1786-7, page 235

APPENDIX A: THE TEMPERATURE DURING COOLING IN THE OWN

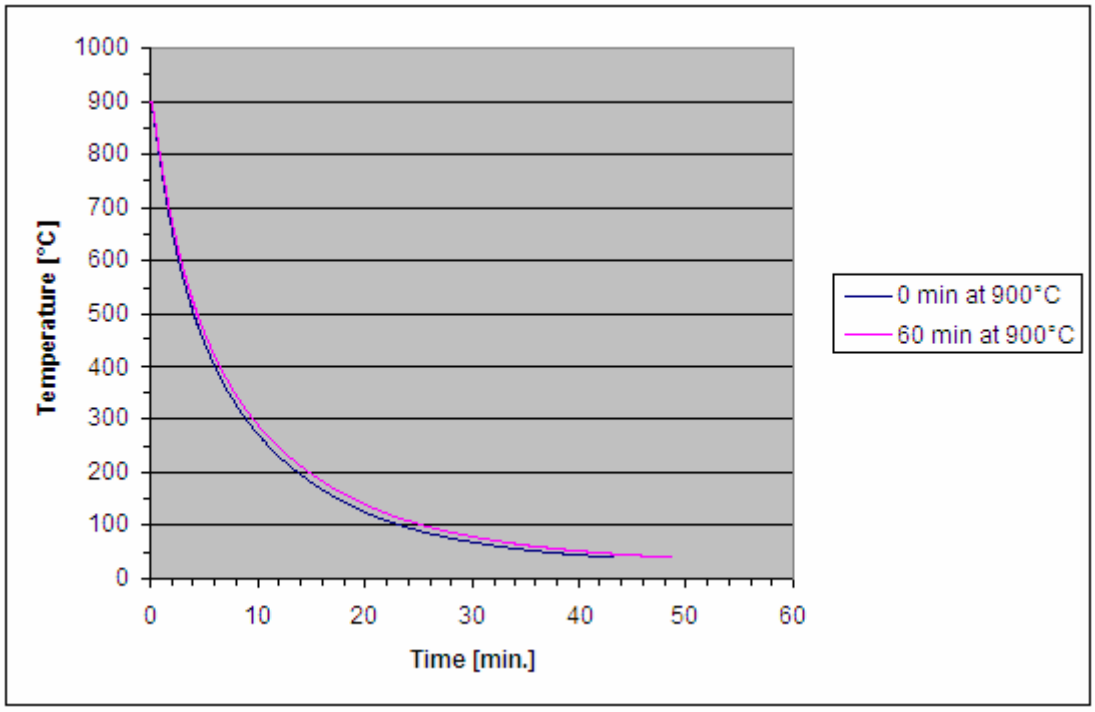

Figure A 1: The temperature during cooling in the own.

APPENDIX B: VURDERING AV NOEN KJEMISKE REAKSJONER

```
1) Noen data for reaktanter og produkter:

Hovedprodukt > Fe
Fe1(cr)
Fe1(g)
Fe1(l)
Fe1+(g)
Fe1-(g)
Smeltepunkt       :=   1816 K
Smeltevarme       :=    13.88 kJ/mol
Kokepunkt         :=   3133 K
Fordampningsvarme:=   349.27 kJ/mol
Skal kokepunktet beregnes for et annet trykk >
```

```
Produkt med faseangivelse > Fe(s)
Hill_formel...: Fe1(cr)
Molekylvekt...:   55.847
Hf............:      -0.00 kJ/mol
Ef............:      -0.00 kJ/mol
Sf............:      27.53 J/mol*K
Td............:   1042 K
Tmax..........:   2200 K

Produkt med faseangivelse > Fe(l)
Hill_formel...: Fe1(l)
Molekylvekt...:   55.847
Hf............:      12.43 kJ/mol
Ef............:      12.43 kJ/mol
Sf............:      34.74 J/mol*K
Td............:   1200 K
Tmax..........:   4000 K

Produkt med faseangivelse > Fe(g)
Hill_formel...: Fe1(g)
Molekylvekt...:   55.847
Hf............:     415.20 kJ/mol
Ef............:     412.73 kJ/mol
Sf............:     180.38 J/mol*K
Td............:   1000 K
Tmax..........:   6000 K

Hovedprodukt > FeO
Fe1O1(cr)
Fe1O1(g)
Fe1O1(l)
Smeltepunkt      :=   1651 K
Smeltevarme      :=    24.06 kJ/mol
Kokepunkt        :=   3839 K
Fordampningsvarme:=   405.39 kJ/mol
Skal kokepunktet beregnes for et annet trykk >

Produkt med faseangivelse > FeO(s)
Hill_formel...: Fe1O1(cr)
Molekylvekt...:   71.846
Hf............:    -271.88 kJ/mol
Ef............:    -270.64 kJ/mol
Sf............:      60.72 J/mol*K
Td............:   1000 K
Tmax..........:   2000 K

Produkt med faseangivelse > FeO(l)
Hill_formel...: Fe1O1(l)
Molekylvekt...:   71.846
Hf............:    -249.38 kJ/mol
Ef............:    -248.14 kJ/mol
Sf............:      75.37 J/mol*K
Td............:   1100 K
```

```
Tmax.........:   5000 K

Produkt med faseangivelse > FeO(g)
Hill_formel...: Fe1O1(g)
Molekylvekt...:   71.846
Hf...........:     250.88 kJ/mol
Ef...........:     249.64 kJ/mol
Sf...........:     241.77 J/mol*K
Td...........:   1000 K
Tmax.........:   6000 K

Produkt med faseangivelse > CO2(g)
Hill_formel...: C1O2(g)
Molekylvekt...:   44.010
Hf...........:    -393.28 kJ/mol
Ef...........:    -393.28 kJ/mol
Sf...........:     213.66 J/mol*K
Td...........:   1000 K
Tmax.........:   6000 K

Produkt med faseangivelse > CO(g)
Hill_formel...: C1O1(g)
Molekylvekt...:   28.010
Hf...........:    -110.46 kJ/mol
Ef...........:    -111.70 kJ/mol
Sf...........:     197.53 J/mol*K
Td...........:   1000 K
Tmax.........:   6000 K

Produkt med faseangivelse > C(s)
Hill_formel...: C1(cr)
Molekylvekt...:   12.011
Hf...........:       -0.00 kJ/mol
Ef...........:       -0.00 kJ/mol
Sf...........:        5.73 J/mol*K
Td...........:   1000 K
Tmax.........:   6000 K

Produkt med faseangivelse > O2(g)
Hill_formel...: O2(g)
Molekylvekt...:   31.999
Hf...........:       -0.00 kJ/mol
Ef...........:       -0.00 kJ/mol
Sf...........:     205.02 J/mol*K
Td...........:   1000 K
Tmax.........:   6000 K

Hovedprodukt > H2O
H2O1(fl)
H2O1(g)
H2O1(l)
Kokepunkt        :=    373 K
Fordampningsvarme:=    40.82 kJ/mol
Skal kokepunktet beregnes for et annet trykk >
```

```
Produkt med faseangivelse > H2O(l)
Hill_formel...: H2O1(l)
Molekylvekt...:   18.015
Hf............:    -285.66 kJ/mol
Ef............:    -281.94 kJ/mol
Sf............:      69.91 J/mol*K
Td............:    500 K
Tmax..........:    500 K

Produkt med faseangivelse > H2O(g)
Hill_formel...: H2O1(g)
Molekylvekt...:   18.015
Hf............:    -241.68 kJ/mol
Ef............:    -240.44 kJ/mol
Sf............:     188.71 J/mol*K
Td............:   1000 K
Tmax..........:   6000 K


2) Termodynamiske koeffisienter

Produkt med faseangivelse > H2(g)
a( 1):=    2.732758&+000
a( 2):=    1.099447&-003
a( 3):=   -2.730907&-007
a( 4):=    3.970450&-011
a( 5):=   -2.336469&-015
a( 6):=   -7.154514&+002
a( 7):=    1.266783&-001
a( 8):=    2.910809&+000
a( 9):=    3.716520&-003
a(10):=   -8.402946&-006
a(11):=    8.199988&-009
a(12):=   -2.794673&-012
a(13):=   -9.736912&+002
a(14):=   -1.679024&+000

Produkt med faseangivelse > N2(g)
a( 1):=    2.970653&+000
a( 2):=    1.370300&-003
a( 3):=   -4.829296&-007
a( 4):=    7.742490&-011
a( 5):=   -4.585867&-015
a( 6):=   -9.338410&+002
a( 7):=    5.753252&+000
a( 8):=    3.743449&+000
a( 9):=   -1.735575&-003
a(10):=    3.707152&-006
a(11):=   -2.151259&-009
a(12):=    3.675136&-013
a(13):=   -1.067643&+003
a(14):=    2.072538&+000
```

```
Produkt med faseangivelse > CO2(g)
a( 1):=    4.598830&+000
a( 2):=    2.780124&-003
a( 3):=   -1.020376&-006
a( 4):=    1.688570&-010
a( 5):=   -1.021756&-014
a( 6):=   -4.897290&+004
a( 7):=   -1.714615&+000
a( 8):=    2.173015&+000
a( 9):=    1.034262&-002
a(10):=   -1.064271&-005
a(11):=    6.231606&-009
a(12):=   -1.575862&-012
a(13):=   -4.832344&+004
a(14):=    1.065267&+001

Produkt med faseangivelse > CO(g)
a( 1):=    3.052704&+000
a( 2):=    1.344791&-003
a( 3):=   -4.850808&-007
a( 4):=    7.939932&-011
a( 5):=   -4.790204&-015
a( 6):=   -1.426008&+004
a( 7):=    5.978075&+000
a( 8):=    3.813442&+000
a( 9):=   -2.389681&-003
a(10):=    5.660183&-006
a(11):=   -4.129409&-009
a(12):=    1.034174&-012
a(13):=   -1.435760&+004
a(14):=    2.524696&+000

Produkt med faseangivelse > H2O(g)
a( 1):=    2.641164&+000
a( 2):=    3.072109&-003
a( 3):=   -8.692926&-007
a( 4):=    1.169281&-010
a( 5):=   -5.990411&-015
a( 6):=   -2.985609&+004
a( 7):=    7.053899&+000
a( 8):=    4.169818&+000
a( 9):=   -1.843379&-003
a(10):=    6.026145&-006
a(11):=   -4.958236&-009
a(12):=    1.566124&-012
a(13):=   -3.027111&+004
a(14):=   -7.392809&-001

Produkt med faseangivelse > O2(g)
a( 1):=    3.898321&+000
a( 2):=    2.996767&-004
a( 3):=    4.242153&-008
a( 4):=   -1.995691&-011
a( 5):=    1.868715&-015
```

```
a( 6):=   -1.328959&+003
a( 7):=    2.031436&+000
a( 8):=    3.807109&+000
a( 9):=   -3.220541&-003
a(10):=    1.047526&-005
a(11):=   -1.040450&-008
a(12):=    3.534313&-012
a(13):=   -1.065602&+003
a(14):=    3.545130&+000
```

Tv og Tp for noen reaksjoner:

1) Fe(s) + CO2(g) = FeO(s) + CO(g)	endoterm
2) Fe(s) + 0.5O2(g)= FeO(s)	Tp=4430K Tv:=4391K
3) Fe(s) + CO(g) = FeO(s) + C(s)	Tp=2261K Tv:=2221K
4) Fe(s) + H2O(g) = FeO(s) + H2(g)	Tp= 666K Tv:= 722K

ΔG(T) ved 1 og 450 bar for:
Fe(s) + CO2(g)
Fe(l) + CO2(g)
FeO(s) + CO(g)
FeO(l) + CO(g)

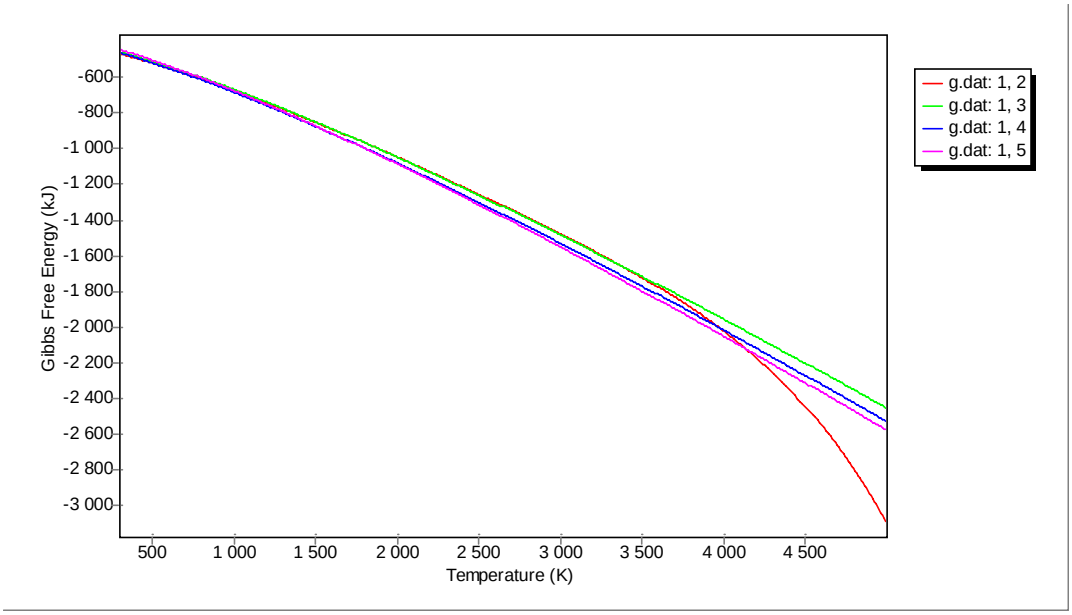

G(T) ved 1 bar

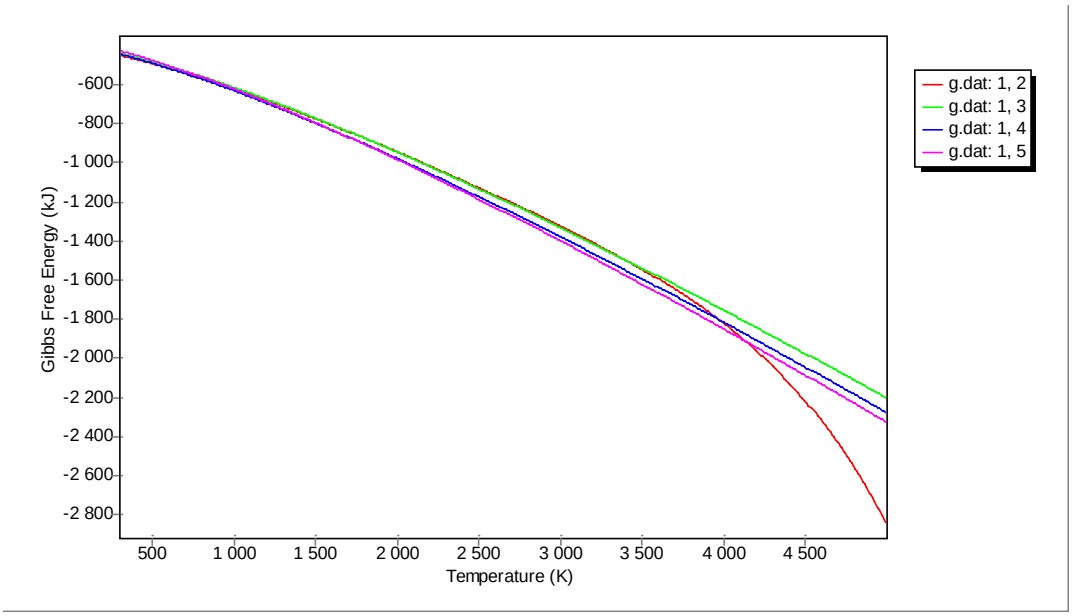

G(T) ved 450 bar

ΔG(T) ved 1 og 450 bar for:
Fe(s) + 0.5O2(g)
Fe(l) + 0.5O2(g)
FeO(s)
FeO(l)

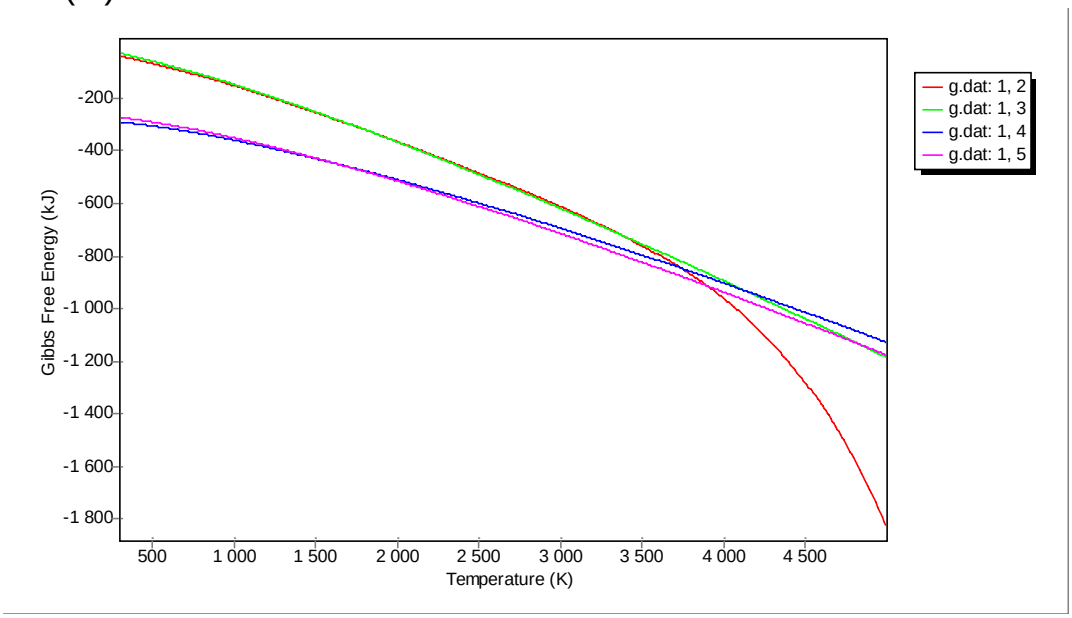

G(T) ved 1 bar

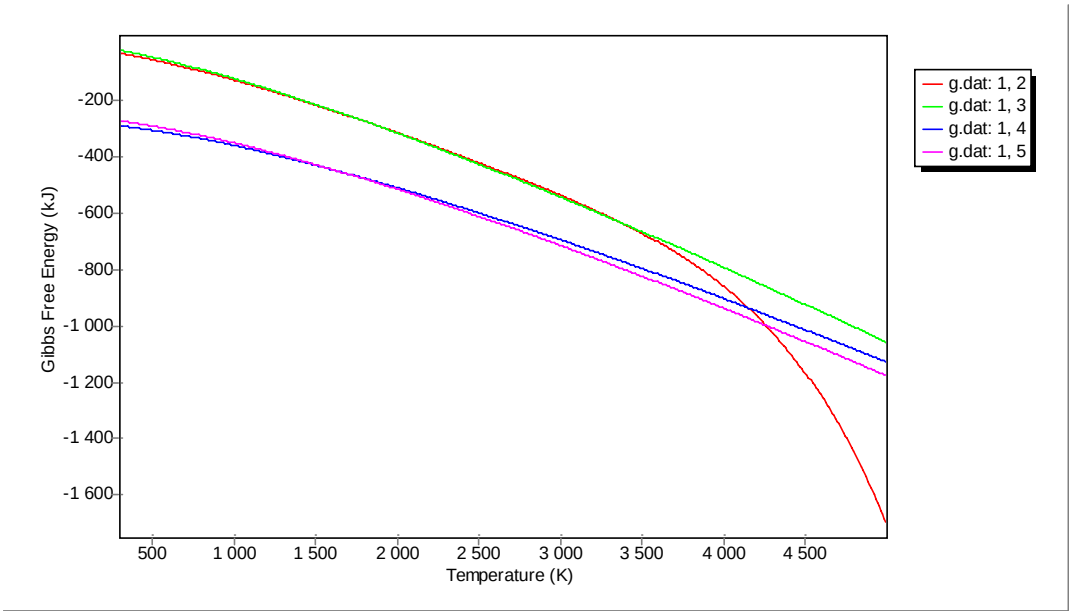

G(T) ved 450 bar

ΔG(T) ved 1 og 450 bar for:
Fe(s) + CO(g)
Fe(l) + CO(g)
FeO(s)+ C(s)
FeO(l)+ C(s)

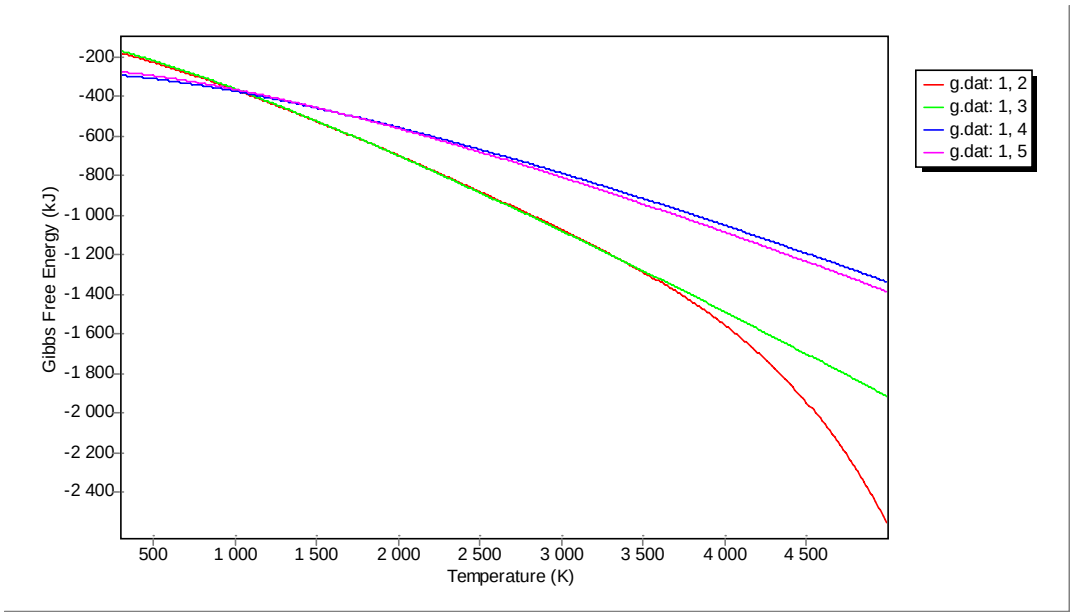

G(T) ved 1 bar

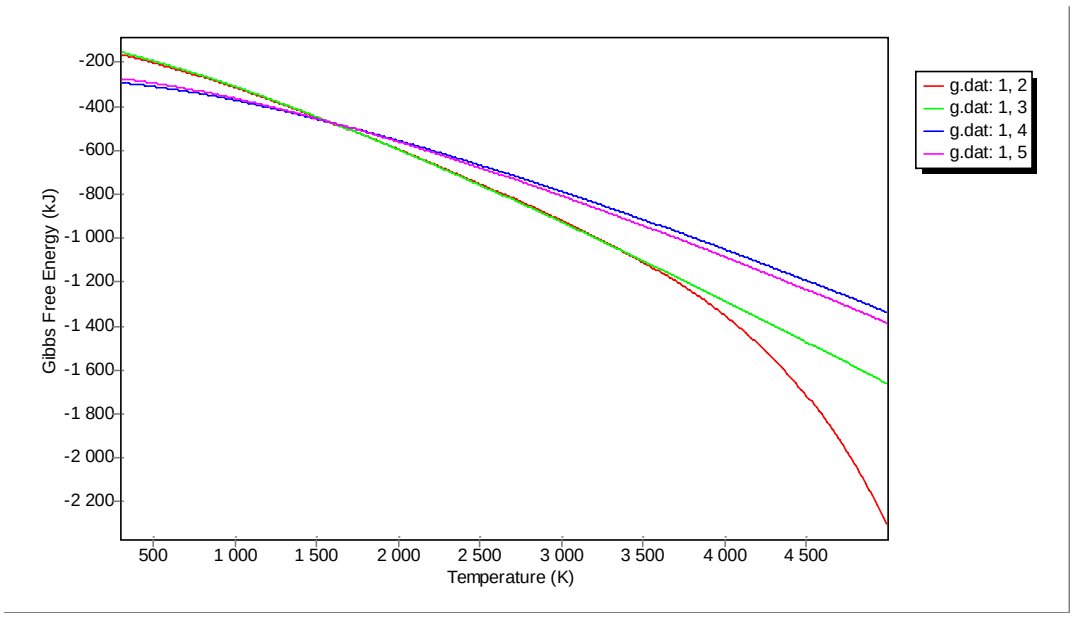

G(T) ved 450 bar

ΔG(T) ved 1 og 450 bar for:
Fe(s) + H2O(g)
Fe(l) + H2O(g)
FeO(s)+ H2(g)
FeO(l)+ H2(g)

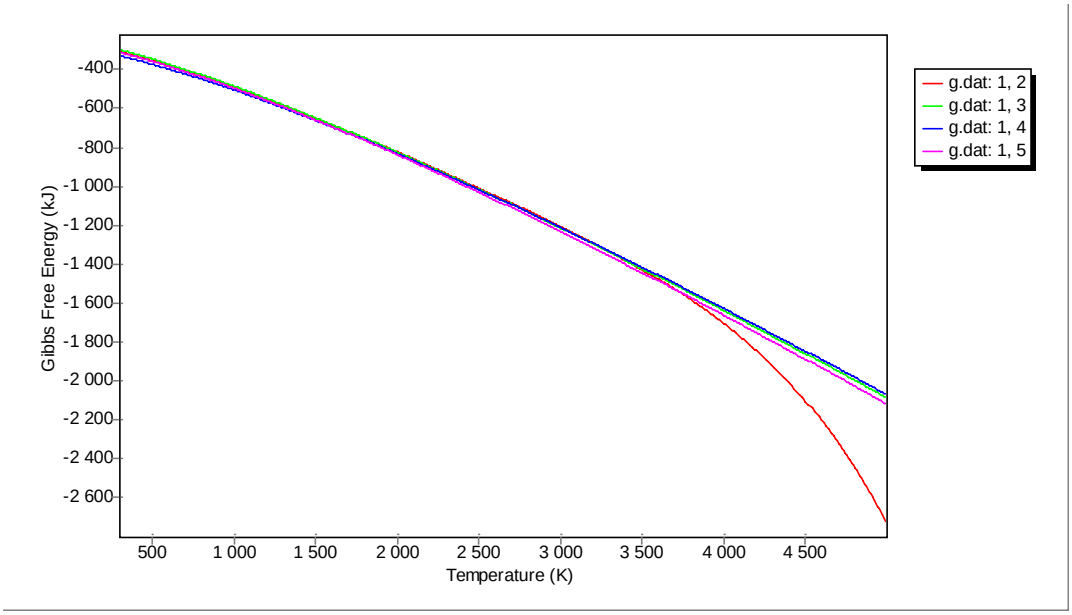

G(T) ved 1 bar

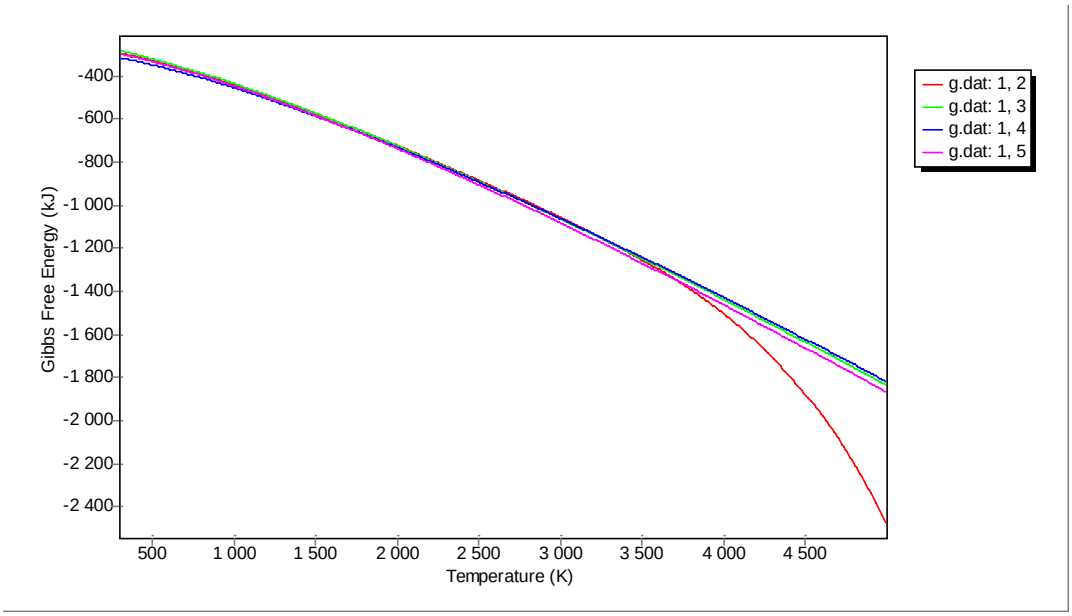

G(T) ved 450 bar

Ved vurdering av resultatene fra disse G(T) diagrammene bør man ta hensyn til Tmax for de forskjellige komponentene.

Tv og Tp for noen reaksjoner:

5) Fe(s) + CO2(g) = FeO(s) + CO(g) endoterm
6) Fe(s) + 0.5O2(g)= FeO(s) Tp=4430K Tv:=4391K
7) Fe(s) + CO(g) = FeO(s) + C(s) Tp=2261K Tv:=2221K
8) Fe(s) + H2O(g) = FeO(s) + H2(g) Tp= 666K Tv:= 722K

APPENDIX C: MPXX6/CPT.SIM BEREGNER HT(T) OG ET(T) FOR PRODUKTBLANDINGER

7)Fe(s) + CO(g) = FeO(s) + C(s)
700 K 2900 K

Ht(Fe(s)+CO(g)) = 12.02 + -20.69 = -8.67 kJ
Gt(Fe(s)+CO(g)) = -24.59+ - 810.06 = -834.65 kJ

Ht(FeO(s)+C(s)) = -8.67 kJ for **T= 4332 K**
Gt(FeO(g)+C(s)) = -1066.92 + -167.52 = -1234.44 kJ
Gt(FeO(g)+C(s)) < Gt(Fe(s)+CO(g))
4332 K 700 K 2900 K

Ht(FeO(l)+C(s) = -8.67 kJ for **T= 4055 K**
kpt for FeO = 3839 ved 1 bar.

Sansynligvis så vil man få en temperatur som maximalt er lik kpt for FeO(l). Kokepunktet for FeO vil ikke være noen begrensning ved 450 bar.

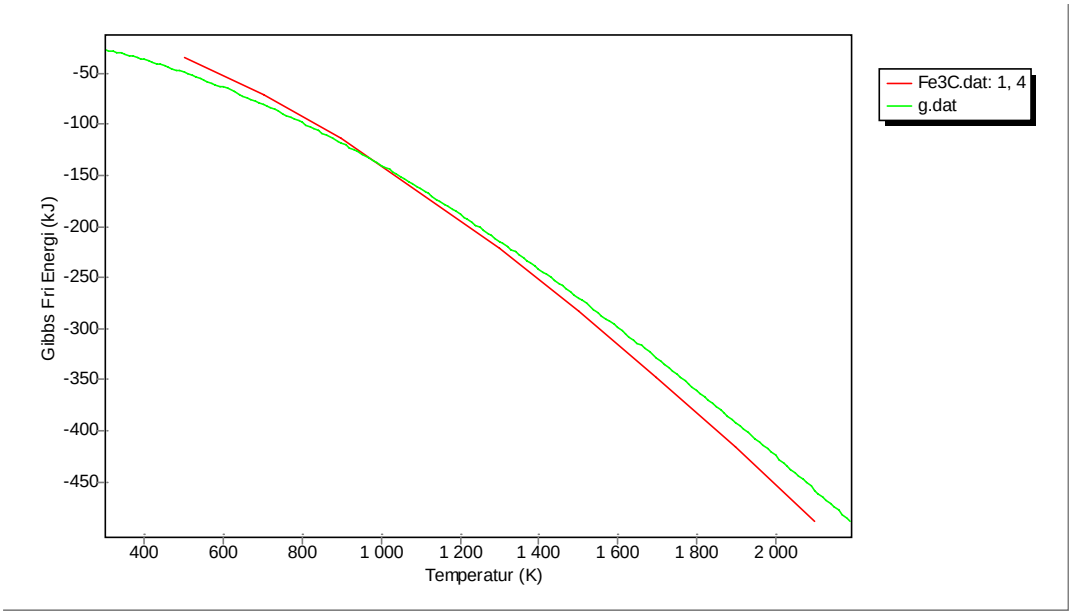

G(T) for Fe3C(s) og 3Fe(s) + C(s)

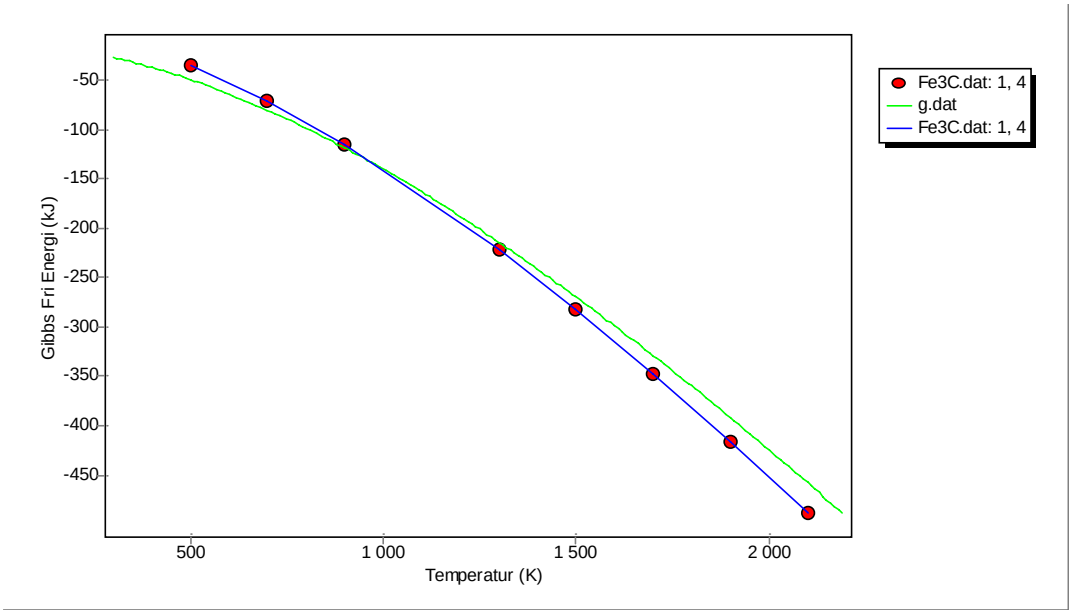

G(T) for Fe3C(s) og 3Fe(s) + C(s)

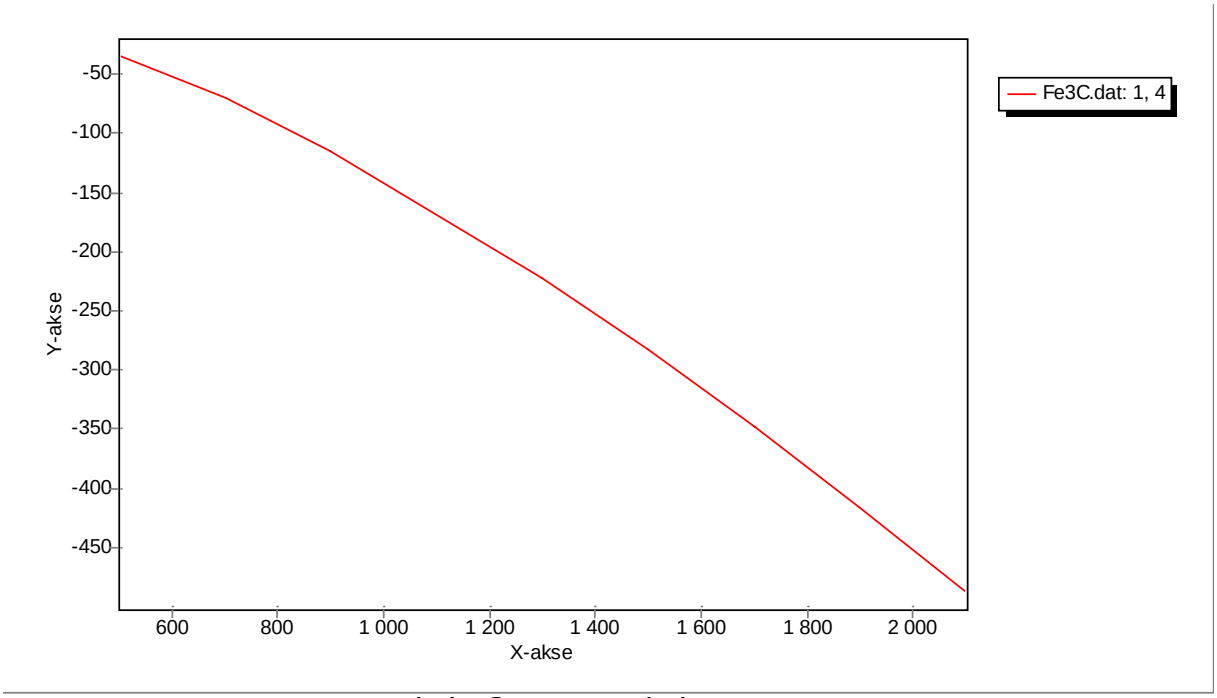

G(T) for Fe3C(s)

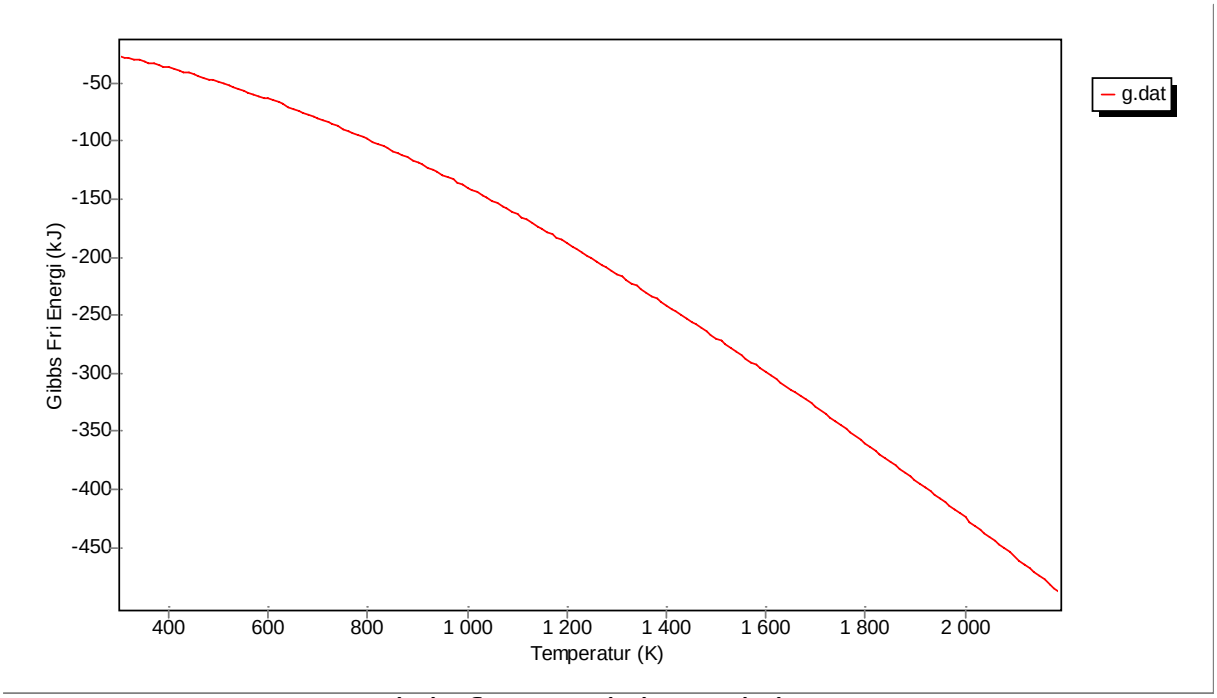

G(T) for 3Fe(s) + C(s)